DEVELOPMENT AND ANALYSIS OF STARTUP STRATEGIES
FOR A PARTICLE BED NUCLEAR ROCKET ENGINE

by

DAVID E. SUZUKI

B.S., Astronautical Engineering
United States Air Force Academy, 1991

Submitted to the Department of Aeronautics and Astronautics
and the
Department of Nuclear Engineering

in Partial Fulfillment of the Requirements for the Degrees of

Master of Science in Aeronautics and Astronautics
and
Master of Science in Nuclear Engineering

at the
Massachusetts Institute of Technology
June 1993

Signature of Author_____
Department of Aeronautics and Astronautics
Department of Nuclear Engineering, April 26, 1993

Certified by_____
Professor Jack L. Kerrebrock, Department of Aeronautics and Astronautics
Thesis Co-Supervisor

Certified by_____
Professor David D. Lanning, Department of Nuclear Engineering
Thesis Co-Supervisor

Accepted by_____
Professor Harold Y. Wachman, Department of Aeronautics and Astronautics
Chairman, Department Graduate Committee

Accepted by_____
Professor Allan F. Henry, Department of Nuclear Engineering
Chairman, Department Graduate Committee

REPORT DOCUMENTATION PAGE

Form Approved
OMB No. 0704-0188

1. AGENCY USE ONLY (Leave blank)	2. REPORT DATE	3. REPORT TYPE AND DATES COVERED
	Jun 1993	THESIS/~~DISSERTATION~~XXX

4. TITLE AND SUBTITLE
Development and Analysis of Startup Strategies for Particle Bed Nuclear Rocket Engine

5. FUNDING NUMBERS

6. AUTHOR(S)

2Lt David E. Suzuki

7. PERFORMING ORGANIZATION NAME(S) AND ADDRESS(ES)

AFIT Student Attending: Massachusetts Institute of Technology

8. PERFORMING ORGANIZATION REPORT NUMBER

AFIT/CI/CIA- 93-088

9. SPONSORING MONITORING AGENCY NAME(S) AND ADDRESS(ES)

DEPARTMENT OF THE AIR FORCE
AIR FORCE INSTITUTE OF TECHNOLOGY/CI
2950 P STREET
WRIGHT-PATTERSON AFB OH 45433-7765

10. SPONSORING MONITORING AGENCY REPORT NUMBER

11. SUPPLEMENTARY NOTES

12a. DISTRIBUTION AVAILABILITY STATEMENT

Approved for Public Release IAW 190-1
Distribution Unlimited
MICHAEL M. BRICKER, SMSgt, USAF
Chief Administration

12b. DISTRIBUTION CODE

13. ABSTRACT (Maximum 200 words)

14. SUBJECT TERMS

15. NUMBER OF PAGES
104

16. PRICE CODE

17. SECURITY CLASSIFICATION OF REPORT	18. SECURITY CLASSIFICATION OF THIS PAGE	19. SECURITY CLASSIFICATION OF ABSTRACT	20. LIMITATION OF ABSTRACT

DEVELOPMENT AND ANALYSIS OF STARTUP STRATEGIES
FOR A PARTICLE BED NUCLEAR ROCKET ENGINE

by

DAVID E. SUZUKI

Submitted to the Department of Aeronautics and Astronautics
and the
Department of Nuclear Engineering

on April 26, 1993 in Partial Fulfillment
of the Requirements for the Degrees of

Master of Science in Aeronautics and Astronautics
and
Master of Science in Nuclear Engineering

Abstract

The particle bed reactor (PBR) nuclear thermal propulsion rocket engine concept is the focus of the Air Force's Space Nuclear Thermal Propulsion program. While much progress has been made in developing the concept, several technical issues remain. Perhaps foremost among these concerns is the issue of flow stability through the porous, heated bed of fuel particles. There are two complementary technical issues associated with this concern: the identification of the flow stability boundary and the design of the engine controller to maintain stable operation. This thesis examines a portion of the latter issue which has yet to be addressed in detail. Specifically, it develops and analyzes general engine system startup strategies which maintain stable flow through the PBR fuel elements while reaching the design conditions as quickly as possible. The PBR engine studies are conducted using a computer model of a representative particle bed reactor and engine system. The computer program utilized is an augmented version of SAFSIM, an existing nuclear thermal propulsion modeling code; the augmentation, dubbed SAFSIM+, was developed by the author and provides a more complete engine system modeling tool. Elements of the startup strategy considered include: the coordinated control of reactor power and coolant flow; turbine inlet temperature and flow control; and use of an external starter system. The simulation results indicate that flow instability is an issue which must be considered in formulating the engine startup strategy. The use of an external starter system enables the engine to reach design conditions very quickly while maintaining the flow well away from the unstable regime. If a bootstrap start is used instead, the transient progresses somewhat slower and approaches closer to the unstable flow regime, but allows for greater engine reusability. These results can provide important information to engine designers and mission planners. In addition, this thesis demonstrates the versatility and robustness of the SAFSIM+ computer model developed to simulate the engine system.

2

Acknowledgements

Table of Contents

List of Figures

List of Tables

Chapter 1 Introduction

1.1 Objective

The particle bed reactor (PBR) nuclear rocket engine concept is the focus of the United States Air Force's Space Nuclear Thermal Propulsion program. While much progress has been made in developing the concept, several technical issues remain. Perhaps foremost among these concerns is the issue of flow stability through the porous, heated bed of fuel particles. There are two complementary technical issues associated with this concern: the identification of the flow instability region and the design of the engine controller to maintain stable operation. The objective of this thesis is to study a portion of the latter issue which has yet to be addressed in detail. Specifically, it is to develop and analyze engine system startup strategies which maintain stable flow through the PBR fuel elements while reaching the design conditions as quickly as possible.

1.2 Nuclear Thermal Propulsion

1.2.1 Concept

Nuclear thermal propulsion (NTP) rocket systems differ from conventional chemical propulsion systems in that they utilize a nuclear reactor rather than a chemical reaction to provide the energy necessary to produce thrust. The reactor coolant fluid removes the thermal energy generated by the reactor and serves as the propellant which is exhausted through the rocket nozzle. NTP systems can achieve significant performance advantages, measured in terms of specific impulse (I_{SP}), over chemical propulsion systems. Specific impulse is defined as the ratio of engine thrust to propellant weight flow rate; the higher the engine specific impulse, the more fuel efficient the rocket system will be. This efficiency can translate into a lower initial vehicle mass for a given mission velocity increment (ΔV), or a greater possible ΔV for a given initial mass. The ideal specific impulse of a rocket system is related to the propellant chamber temperature and molecular mass according to: $I_{SP} \propto \sqrt{T_c/M}$. The most advanced chemical propulsion systems, using cryogenic oxygen and hydrogen, are limited in efficiency to about 475 *sec* I_{SP} due to the requirement for relatively heavy, combustible propellants. NTP systems,

11

however, do not have this limit. Therefore, the preferred propellant for NTP systems is hydrogen, which has a very low molecular mass. The chamber temperature--which is actually the reactor coolant exit temperature--for solid-core NTP systems is limited to about 3000 K by the solid material properties. An NTP system using hydrogen at 3000 K has an ideal specific impulse of approximately 1000 *sec*. The performance advantage gained by this increase in efficiency is shown in Figure 1.1. The figure compares the payload fraction of ignition mass as a function of the mission ΔV requirement for an NTP system and both a cryogenic (liquid oxygen/liquid hydrogen) and hypergolic (nitrogen tetroxide/monomethyl hydrazine) chemical system. Included on the graph is the ΔV requirement for a typical low earth orbit (LEO) to geosynchronous equatorial orbit (GEO) orbital transfer vehicle (OTV) mission and the range of mission energies for which nuclear thermal propulsion is mission enabling. The calculations assume that the entire ΔV is provided by a single rocket stage.

Figure 1.1 Performance Advantage of Nuclear Thermal Propulsion [S-2]
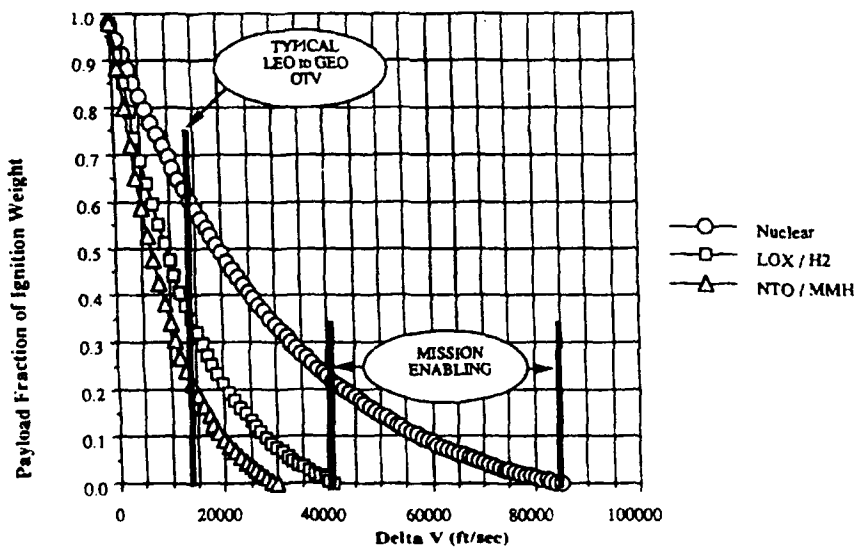
1.2.2 History

Nuclear thermal propulsion was originally studied and developed through ground demonstration during the Nuclear Engine for Rocket Vehicle Applications (NERVA)

program from 1955 to 1972, at which point the program was phased out along with the Apollo program. The NERVA program designed, built, and tested several engine designs. Table 1.1 summarizes key performance parameters achieved during the program [K-2].

Table 1.1 Maximum Performance Achieved by NERVA Program

Parameter	Engine	Value Achieved
Power	PHOEBUS-2A	4100 *MW*
Thrust	PHOEBUS-2A	930 *kN*
Specific Impulse	PEWEE	845 *sec*
Chamber Temperature	PEWEE	2750 *K*
Total Time at Full Power	NF-1	109 *minutes*
Number of Restarts	XE	28

Recently, NTP rocket engines have received much renewed attention due to the greatly improved performance which they offer. NTP systems have been identified as a key technology for the Space Exploration Initiative since they can greatly reduce the trip time needed for a manned mission to Mars [S-1]. Nuclear propulsion systems have also been investigated as part of the Strategic Defense Initiative and by the Air Force for use as an upper stage for a launch vehicle, as an orbital transfer vehicle, and for various other missions.

1.2.3 Particle Bed Reactor

1.2.3.1 Concept

The particle bed reactor is a new reactor concept originated by Brookhaven National Laboratory [P-2]. This reactor is the focus of the Air Force's Space Nuclear Thermal Propulsion program. Unlike the NERVA reactors, in which the propellant flowed axially through coolant passages in long, hexagonal fuel elements, the propellant in the PBR

13

flows radially through a porous bed of small (~500 µ) fuel particles. This configuration increases the surface area available for heat transfer from the fuel to the hydrogen coolant, thus increasing both the maximum possible coolant temperature and the maximum possible reactor power density. The PBR has a nominal fuel volume power density of about 40 GW/m^3 compared to a maximum of only 5.2 GW/m^3 for the NERVA reactors. The high power density greatly reduces the size of the PBR engine compared to the relatively large and heavy NERVA engines, which leads to a higher engine thrust-to-weight ratio. This advantage makes the PBR concept particularly attractive to the Air Force, especially for small, high-energy missions.

Figure 1.2 PBR Fuel Element Design [B-2]
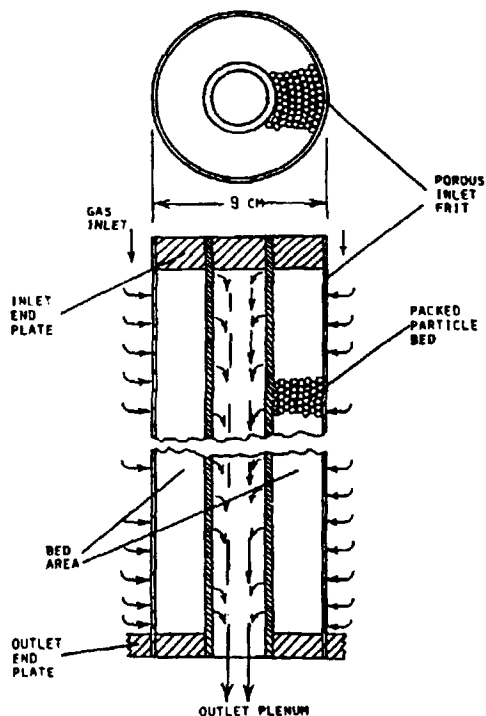
1.2.3.2 Basic Design

The PBR core consists of multiple fuel elements (the number is dependent on the desired power level or thrust) arranged in an hexagonal pattern. The fuel elements are embedded in a moderator and contained within a pressure vessel. Each fuel element is annular in shape, and may be tapered axially. The bed of fuel particles is contained between two

14

porous frits. The hydrogen coolant enters the inlet plenum from the moderator cooling passages and then flows radially through the cold frit, the packed bed of fuel particles, and the hot frit. The hot coolant then turns and flows down the outlet plenum to a chamber where the flows from each element are mixed and then exhausted through a rocket nozzle. Figure 1.2 shows a representative fuel element design.

1.2.3.3 Technical Issues

Much progress has been made in developing the PBR concept, including work on reactor physics, fuel fabrication, and testing of individual fuel elements. However, some technical issues remain to be resolved in the continuing development of this novel reactor concept. Perhaps foremost among these concerns is the issue of flow instability through the porous, heated bed of fuel particles.

1.3 Flow Instability

1.3.1 Description

The possibility for flow instability in a PBR fuel element exists due to the multiple flow paths which the coolant may take once it enters the porous, heated bed of fuel particles. The mechanism for the instability can be outlined as follows [M-1,W-3]:

   a) multiple flow paths through a heated medium are connected at plenum regions with fixed inlet pressure and temperature and fixed outlet pressure;

   b) a perturbation in one flow path causes the temperature to rise, thus increasing the fluid viscosity and reducing the fluid density;

   c) since the pressure drop is fixed by the plena, the mass flow in this path will decrease;

   d) the reduction in mass flow will result in a higher fluid temperature in this flow path, assuming the heat generation remains constant;

   e) this process could continue until the temperature exceeds failure limits for the fuel element.

The location of the flow stability boundary for a particular fuel element geometry has not yet been well established, but experimental, analytical and numerical analyses are

currently being conducted at MIT and other organizations. In addition, the exact nature of the instability is not yet fully understood. However, Lawrence [L-1] has shown that an instability appears to exist near the regions predicted by several different analyses.

1.3.2 Boundary Identification Methods

1.3.2.1 Maise

The method used by Maise [M-1] to identify the flow instability regime is an adaptation of the well-known Bussard and DeLauer parallel channel analysis [B-4]. This method assumes simple relations for hydrogen properties as a function of temperature, and assumes that the multiple flow paths are one-dimensional parallel channels. The Ergun relation is used to calculate the pressure drop through the packed bed of fuel particles. The neutral stability criterion is defined as the minimum point of pressure drop as a function of coolant flow rate for a particular fuel element power density. The locus of these minima over the range of possible power densities then forms the neutral stability line which separates the stable and unstable flow regimes.

1.3.2.2 Witter

Witter [W-3] uses a method and criterion similar to that of Maise, but uses more accurate hydrogen property data and actual fuel element dimensions. The hydrogen properties are based on National Bureau of Standards properties for para-hydrogen. Witter also uses the Ergun relation, but calculates the pressure drop by numerically integrating the applicable equations over the thickness of the fuel bed.

1.3.2.3 Kerrebrock & Kalamas

Kerrebrock and Kalamas [K-1] use a completely different method than those of Maise and Witter. This method is based on the three-dimensional momentum and energy equations for the coolant using approximate relations for the hydrogen properties as a function of temperature. The effect of conductivity within the bed is also included in the analysis. To simplify the calculations, they assume a planar rather than a cylindrical

16

geometry. Kerrebrock and Kalamas use a stability criterion based on the growth or decay of harmonic perturbations introduced into the bed.

1.3.3 Stability Map

The stability boundaries calculated by the methods of Maise, Witter, and Kerrebrock and Kalamas are shown in Figure 1.3. The plotted curves show the element temperature rise ratio, $\Phi = \dfrac{T_{out} - T_{in}}{T_{in}}$, as a function of the superficial Reynolds number at the bed inlet which results in nuetrally stable flow. The superficial Reynolds number is defined as: $Re_s = \dfrac{\dot{m} \cdot d}{A \cdot \mu}$ where $\dot{m}$ is the fluid flow rate, d is the fuel particle diameter, A is the total cross-sectional flow area (particles and voids), and μ is the fluid viscosity. The region above each curve represents the operating regime where the possibility for flow instability exists.

Figure 1.3 Flow Stability Boundaries
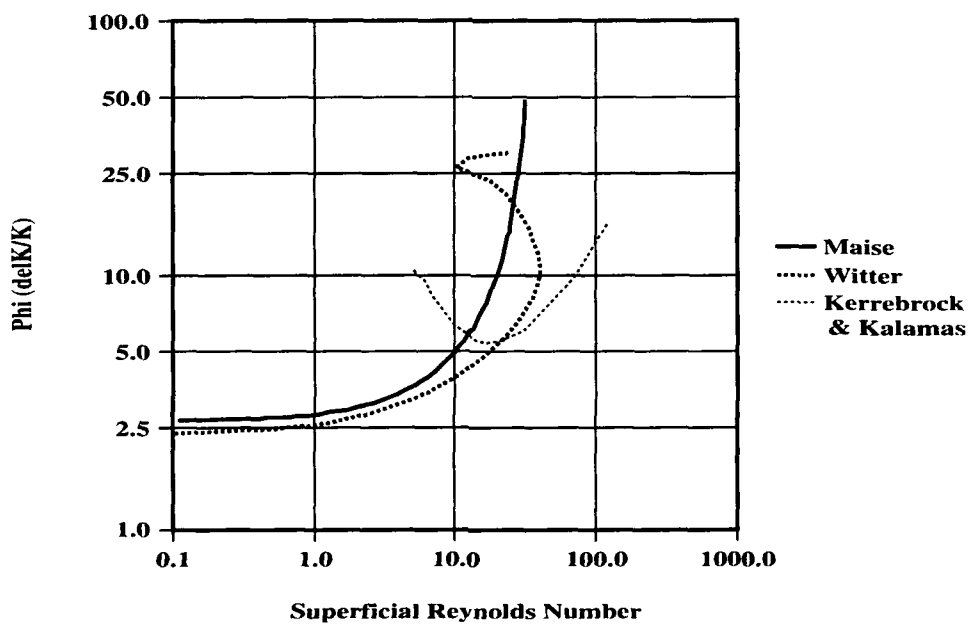
While the curves are somewhat different based on the differing methodologies, they show that flow instability can be expected during low flow but high temperature operation. The analysis of Kerrebrock and Kalamas predicts that the stability is actually enhanced at

17

Reynolds numbers below approximately 17; this effect is due to the conductivity in the bed region which tends to dissipate heat, thus abating the growth of hot spots in the bed. Low flow but high temperature operation may be expected during startup or shutdown of the engine system; this possibility requires that proper control strategies be developed to ensure that the flow through the fuel elements is maintained in the stable flow regime. It should be noted at this point that a more precise understanding of the instability phenomenon and more accurate modeling will be needed to further refine the location of the instability region. In addition, the flow characteristics which determine stability are dependent on the coolant distribution and the heat generation in each element, which may vary significantly among the fuel elements in the reactor core and may also vary over the operating life of the engine.

1.4 Organization of the Report

This report is divided into five (5) chapters. Chapter 1 has been an introduction, providing the necessary background information on nuclear thermal propulsion, the particle bed reactor, and the issue of flow instability in PBR fuel elements. Chapter 2 describes the computer model used to simulate the particle bed reactor engine system. Additional information on the computer model is presented in Appendices A and B. Chapter 3 provides a description of the nominal PBR engine system model used for this study. Chapter 4 describes the general control framework for the system and the development of the engine system startup strategies, and analyzes the performance of these strategies based on the simulation results. Additional results of the simulations are provided in Appendices C and D. Chapter 5 summarizes the findings of this thesis, draws appropriate conclusions, and makes several recommendations based on the results of this work.

Chapter 2 Computer Model

2.1 General Requirements

The development and analysis of the startup strategies for this thesis were conducted using computer modeling and simulation of a nominal particle bed reactor engine system. In order to accomplish the objective, a simulation and modeling code was needed which captures the key aspects of the system--that is, those aspects which most affect the dynamic response of the system during startup. The general requirements for the system model were determined to be the ability to:

a) model transient thermal hydraulics, heat transfer and reactor dynamics for the particle bed reactor;

b) model the transient response of remaining engine system components such as the turbopump assembly, flow control valves, nozzles, and an external starter system;

c) implement user-defined reactor power control laws;

d) implement user-defined flow control laws.

In addition, it was desired that the simulation code allow for relative ease in modifying the syst. n model and control algorithms.

2.2 System Analysis Flow SIMulator

2.2.1 Background

The System Analysis Flow SIMulator (SAFSIM) program is a FORTRAN program developed at Sandia National Laboratories [D-1]. This program was developed to simulate the integrated performance of systems involving fluid mechanics, heat transfer, and reactor dynamics. Because of its suitability for modeling nuclear thermal propulsion systems which necessarily include all three of these phenomena, the SAFSIM code has been chosen by the NASA/DOE/DOD interagency team as the base computational engine for an NTP system model [W-2]. The fluid mechanics and heat transfer portions of the SAFSIM program have been successfully benchmarked to NERVA NRX/EST test data [L-2].

19

2.2.2 Physics Modules

The SAFSIM computer program contains three basic physics modules: fluid mechanics, heat transfer, and reactor dynamics. Each module solution is advanced individually, but all are coupled at each system timestep via convection, heat generation and reactivity feedback effects. The parameters of each module can be fully specified by the user through the SAFSIM input file.

2.2.2.1 Fluid Mechanics Module

The fluid mechanics module uses a one-dimensional finite-element solution method. It solves the quasi-steady, compressible thermal and mechanical energy equations using: combined momentum and mass continuity; advection, conduction, and convection within the fluid; and an extensive library of pressure drop and heat transfer coefficient correlations. The basic finite-element is described by the inlet, outlet, and average flow areas, the flow length, the hydraulic diameter, and the pressure drop correlation. In addition to this basic finite element, special elements exist which model: a porous media element using either the Ergun or Achenbach correlation; a distributed flow element which allows flow to enter or exit along its length rather than only at the ends; a compressor/pump element using characteristic pump maps; and a choked-flow element based on compressible, isentropic flow. The fluid properties are specified by the user using either functional relations or supplied databases. The hydrogen properties chosen were National Bureau of Standards properties for para-hydrogen [W-1]. These data provided the most accurate data over the wide temperature range encountered during startup of the engine system. However, since the SAFSIM program uses pressure and temperature as the inputs to the fluid properties routine, there is no possibility of simulating two-phase flow; even a homogeneous equilibrium model is not possible. This places a limit on the minimum fluid temperature which can be modeled.

2.2.2.2 Heat Transfer Module

The heat transfer module uses a one-dimensional finite element solution. It allows for the specification of the element geometry and multiple heat exchange surfaces for both

20

convective and radiative coupling of the heat transfer solution to the fluid mechanics solution. The heat generation rate in the elements can also be specified, and can be a function of the reactor power in order to couple the solution to the reactor dynamics module. The finite-element material properties including specific heat and conductivity are user-defined, and can be functions of temperature.

2.2.2.3 Reactor Dynamics Module

The reactor dynamics module uses a point-kinetics solution to model the reactor neutronic power dynamics. Reactivity feedback terms can be specified as any function of any variables calculated by either the fluid mechanics or heat transfer modules, allowing the reactor dynamics solution to be coupled to the other solutions. Any number of delayed neutron groups and decay heat groups can be specified, including the effective fractions, time constants, and initial concentrations for each group. The reactor control law is user supplied and can be modified as required.

2.2.3 Function Controlled Variables

The SAFSIM program includes the capability for function controlled variables, which allows almost any model parameter to be specified as a function of any other model parameters or variables. This very powerful feature allows, for example, the implementation of flow control laws by varying an element flow area based on a node pressure. In addition to a library of available functions, user-defined functions can also be implemented. The importance of this feature will be discussed in section 2.4.

2.2.4 Limitations

There are two limitations to the current version of the SAFSIM program which restrict its usefulness for modeling entire particle bed reactor engine systems during startup. The first limitation is the quasi-steady-state solution used for modeling the fluid mechanics of the system. This makes it difficult, but not impossible, to model components such as an external starter system whose performance is heavily dependent on mass accumulation and pressure buildup in the main system. The second limitation is the lack of a turbine or

integrated turbopump assembly (TPA) element. The performance of the TPA is key during startup since it controls the coolant flow through the entire system. This limitation is more severe than the first and necessitates the augmentation of the SAFSIM program with a model capable of simulating the TPA performance.

2.3 Nuclear Thermal Propulsion SIMulator

2.3.1 Background

The Nuclear Thermal Propulsion SIMulator (NTPSIM) is a FORTRAN computer program developed by the author by modifying the ENGine SIMulator (ENGSIM) code previously used at Grumman Electronic Systems Division to model the performance of NTP systems. The modifications include modularization of the code and improvement of certain element modules. The modularization enables the code to model many different engine cycles rather than the particular cycle for which ENGSIM was developed. Improvements to the element modules include a more realistic formulation for the coolant temperature rise within the reactor core, the addition of a more complete neutronic power controller, correction of a few small errors, and conversion to metric units. In addition, a variable step size, stiff-equation integration package was added to replace the fixed step size Runge-Kutta integrator.

2.3.2 Program Elements

2.3.2.1 Fluid Mechanics

The NTPSIM program consists primarily of a simplified dynamic flow simulator which includes the mass accumulation term due to unsteady flow. The framework for the fluid mechanics solution is essentially a series of alternating 'resistor' and 'capacitor' finite elements. The resistor elements include orifices, valves and check valves; capacitor elements include tanks, ducts, flow splitters, and flow mixers. In addition, a turbopump assembly model and a reactor model (discussed below) are included. The system model to be studied can be constructed using any combination of the above elements. The resistor elements determine the mass flow into and out of the adjacent capacitor elements based on the pressure difference between the two elements and the effective flow area of

the resistor element; the governing equations are based on compressible flow through orifices. Capacitor elements calculate the time rate of change of pressure and pressure divided by temperature in the element due to mass accumulation and heat transfer into the element; the governing equations are based on conservation of energy and use ideal gas law relations. Multiple fluids can be specified at different points within the system; ideal gas properties are used for each fluid.

2.3.2.2 Turbopump Assembly Model

The turbopump assembly model includes a coupled pump model and turbine model. The pump performance is based on similarity maps for the pump pressure rise and the required pumping power. The maps provide relations for $\dfrac{\Delta P/N^2}{|\Delta P/N^2|_D}$ and $\dfrac{SHP/N^3}{|SHP/N^3|_D}$ as known functions of $\dfrac{Q/N}{|Q/N|_D}$, where N is the TPA speed, ΔP is the pump pressure rise, *SHP* is the required shaft power, Q is the pump volume flow rate, and D signifies the pump design point conditions. These maps allow the pump pressure rise and required shaft power to be calculated from the pump flow rate and the TPA speed without modeling the complex fluid mechanics within the pump. The pump flow rate is determined by assuming quasi-steady flow through the pump and pump discharge valve such that the pump pressure rise for the given flow and TPA speed is consistent with the driving pressure necessary to produce the same mass flow through the pump discharge valve. The power generated by the turbine is determined using isentropic expansion relations to calculate the ideal temperature change, and hence enthalpy change, across the turbine. This change is then modified appropriately using a turbine efficiency versus flow rate map. The efficiency map relates $\dfrac{\eta}{\eta_D}$ to the normalized spouting ratio, $\dfrac{U/C}{|U/C|_D}$, where η is the turbine efficiency, U is the turbine blade tip speed, C is the mach velocity at the turbine inlet, and D denotes the design conditions. The difference between the turbine power output and the required pumping power is the power available to accelerate the TPA. In this manner, the dynamic response of the TPA can be effectively simulated.

2.3.2.3 Reactor Model

The reactor model used by the NTPSIM code is a very simplistic lumped fluid mechanics and heat transfer model, with a single finite element for the moderator and a single element for the fuel section. The reactor dynamics solution uses point-kinetics. Because of this simplicity, the NTPSIM code was deemed inappropriate for modeling the complex fluid mechanics and heat transfer phenomena present in a particle bed reactor core.

2.3.2.4 Control Laws

The NTPSIM program includes a user-defined subroutine for specifying control laws for any variable in the system model. Typically, this feature would be used to specify the demanded flow area for system valves in order to simulate flow control algorithms.

2.4 SAFSIM+

2.4.1 Description

The SAFSIM+ program was developed by the author and is designed to incorporate the best features of both the SAFSIM program and the NTPSIM program since neither was deemed capable of individually simulating all the key features of a particle bed reactor engine system during startup. The SAFSIM+ program maintains all portions of the SAFSIM code and links it with the NTPSIM code, excluding the reactor model. This augmented version of the SAFSIM code is capable of modeling both the coupled fluid mechanics, heat transfer, and reactor dynamics within the PBR core and the dynamic response of the remainder of the engine system including the turbopump assembly and starter system.

2.4.2 Model Coupling

The two portions of the SAFSIM+ model are coupled at the boundaries of the reactor model. The extent of the reactor portion of the model is arbitrary, but should include as much of the system as possible since the fluid mechanics, fluid property, and heat transfer models of the SAFSIM program are more accurate than those of the NTPSIM model. At each system time step, the SAFSIM reactor model calculates the coolant flow rate

24

through the reactor and the coolant outlet temperature based on the inlet temperature and the inlet and outlet pressure boundary conditions imposed on the reactor. The NTPSIM portion of the model then uses the reactor coolant flow rate and exit temperature to update the pressure and temperature at the boundary elements.

2.4.3 Program Structure

The linkage of the NTPSIM code into the SAFSIM code to create the SAFSIM+ program was accomplished via the function controlled variable (FCV) and user-defined function capabilities built into the SAFSIM program. The inlet and outlet boundary conditions for the reactor portion of the model are specified as FCVs for the system; these variables are updated at each system time step using user-defined functions. The user-defined function structure includes the specification of inputs to the functions; the reactor coolant flow rates and exit temperature required by the NTPSIM code are identified in this manner. A subroutine is provided with the SAFSIM code for specification of the user-defined functions. To create the SAFSIM+ program, this subroutine includes the logic for calling the NTPSIM variable step size integration routine and transferring the data between the NTPSIM and SAFSIM portions of the program using additional common blocks. The remaining NTPSIM subroutines are then simply linked with the SAFSIM subroutines using a FORTRAN compiler and linker. The input data for the NTPSIM portion of the engine system model is incorporated into the SAFSIM+ program using the User-Defined Input block of the standard SAFSIM input file.

2.4.4 Additional Information

Additional information on the SAFSIM+ program is included in Appendices A and B. Appendix A contains a record of slight modifications to the SAFSIM code necessary to implement the SAFSIM+ program and model the PBR engine system. These changes do not include substantive changes to the physics modules or solution methods. Appendix B contains a User's Manual for the SAFSIM+ program.

Chapter 3 System Description

3.1 Engine System

3.1.1 Basic Design Parameters

The engine studies in this thesis are conducted for a representative particle bed reactor nuclear thermal propulsion engine system. The engine is designed for a nominal orbital transfer vehicle mission requiring approximately 100 kN thrust. Hydrogen is chosen for the propellant, with a design operating condition of 7.0 MPa and 3000 K just upstream of the main rocket nozzle; this point in the system will be referred to as the 'chamber' for consistency with chemical rocket propulsion technology which uses the term 'combustion chamber'. This system requires a 500 MW reactor to achieve the desired thrust level.

3.1.2 Engine Cycle

3.1.2.1 Hot Bleed Cycle

A hot bleed cycle is chosen for the orbital transfer vehicle mission since most PBR studies have focused on this engine cycle. Expander cycles are generally not desirable for PBR applications since they require complicated flow paths to extract the energy necessary to drive the turbopump assembly. A schematic diagram of the hot bleed cycle is shown in Figure 3.1. The cycle uses a mixture of hot gas bled from the chamber and cold gas (actually supercritical fluid) from the pump discharge plenum to drive the TPA. The system includes a carbon-carbon composite main rocket nozzle so that regenerative cooling of the nozzle is not necessary.

The engine system model, as shown in Figure 3.1, is simplified to include only those portions of an actual engine system which are most likely to affect the system response during startup. The coolant/propellant is stored at constant pressure and temperature in the hydrogen tank. The hydrogen pressure is then increased by the pump side of the TPA; flow through the pump is controlled by the pump discharge valve (PDV). The coolant then enters the pump discharge plenum where it is split into two flow paths. The main coolant flow enters the reactor and is heated in the moderator and fuel sections. The

majority of this flow is exhausted through the main rocket nozzle, providing the primary thrust for the system. The remainder of the flow from the pump discharge plenum is combined with bleed flow from the chamber in a mixing region. The amount of cold flow from the pump discharge plenum is controlled by the turbine temperature control valve (TCV); the hot bleed flow from the reactor is controlled by the bleed valve (BV). The combined flow then passes through the turbine speed control valve (SCV) and enters a small mixing region; this region also accepts flow from an external starter system. In order to prevent starter gases from entering the reactor, a check valve is included at the SCV location. The combined flow in this mixing region then expands through the turbine, creating shaft power to turn the TPA. Gas from the turbine collects in the turbine exhaust duct and is then expelled through the turbine exhaust nozzle, creating a small amount of thrust.

Figure 3.1 Engine Cycle Schematic
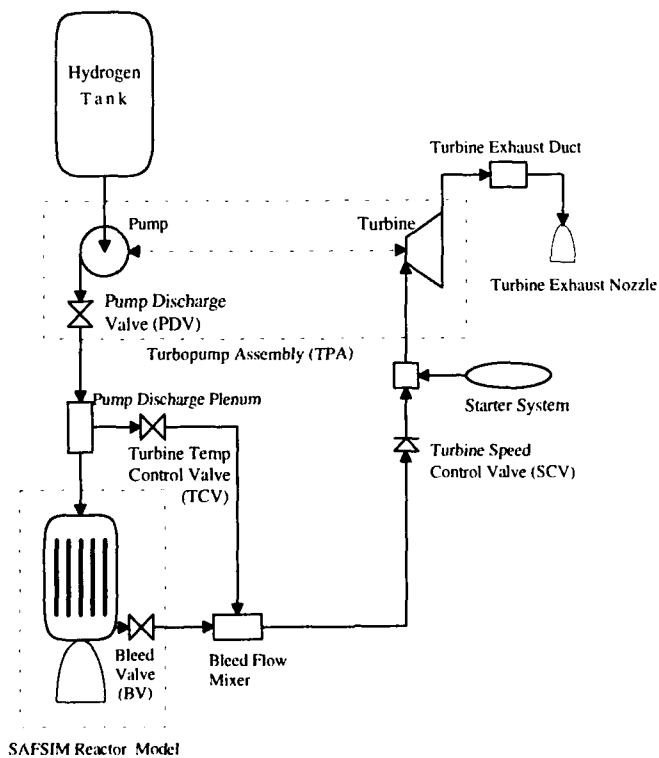
3.1.2.2 Design State Points

Table 3.1 provides the chosen design state points at different locations throughout the engine system.

Table 3.1 Engine System Design State Points

System Location	Pressure (*MPa*)	Temperature (*K*)
Hydrogen Tank	0.3447	50
Pump Outlet	8.2379	52.91
Pump Discharge Plenum	7.8933	52.91
Chamber	7.0	3000
Bleed Flow Mixer	6.454	1800
Turbine Inlet	5.95	1800
Turbine Exhaust Duct	0.3967	1363.64

The hydrogen tank temperature for the model was chosen to be 50 *K* even though the tank temperature for an actual engine is likely to be about 25 *K* in order to maintain the hydrogen propellant in a liquid state. This change was made for two reasons associated with the limits of the SAFSIM program. First, as previously mentioned, the SAFSIM program has no mechanism for simulating two-phase fluid flow, which does occur for temperatures in the range of 25-50 *K* at low pressures. Second, even when single-phase conditions exist in the 25-50 *K* range, the fluid properties may change very rapidly as a function of temperature. In this regime of very sharp negative slopes for some fluid properties, it was found that the SAFSIM solution method had difficulty converging. By initially starting the hydrogen at 50 *K*, these difficulties are averted. Although this change will have a slight effect on system performance (e.g. pressure drops through the core may be slightly different), it is not expected to affect the nature of the overall system startup response.

The pump discharge plenum pressure is based on the design point pressure drop through the reactor core, this is discussed in more detail in section 3.2.4. The pump outlet pressure is calculated from the pump discharge plenum pressure and the pressure drop through the pump discharge valve; the pressure drop is designed to equal the tank pressure so that the required pump pressure rise is equal to the reactor inlet pressure. The temperature rise between the tank and pump outlet is due to the pump efficiency. The design turbine inlet temperature is assumed to be 1800 K, which also sets the bleed flow mixer temperature. No heat loss is modeled over the length of piping between the bleed flow mixer and the turbine, although such losses are expected in an actual engine system. The bleed flow mixer and turbine inlet pressures are chosen to be 92.2% and 85% of the chamber pressure, respectively. The turbine exhaust pressure is based on a 15:1 expansion ratio turbine; the turbine exhaust temperature is calculated from the turbine expansion ratio and the turbine efficiency.

3.1.2.3 Starter System

The engine model includes an external starter system located just upstream of the turbine inlet. This system may be used to initially accelerate the TPA before substantial bleed flow is available from the chamber. Such a system typically consists of a small solid rocket motor which exhausts its propellant into the turbine inlet. This system is modeled as a tank with fixed pressure and temperature and an adjustable check valve. The pressure and valve flow area can be adjusted to simulate a particular solid rocket motor system. The valve flow area can be changed as a function of time to simulate a system with a non-constant mass flow rate; the valve area is set equal to zero for all times after burnup of the solid rocket motor. If an engine system without a starter system is desired, the valve flow area can simply be set to zero so that the same engine model can be used.

3.1.2.4 Fluid Properties

The NTPSIM portion of the SAFSIM+ computer model used to simulate the engine system uses ideal gas properties for each fluid type as discussed in Chapter 2. Table 3.2 lists the fluid properties used for both the hydrogen coolant [G-2] and the starter system

exhaust gas [T-1]. Note that the fluid density provided is the liquid density and is only used by the pump model.

Table 3.2 Engine Fluid Properties

Property	Hydrogen	Starter Gas
Choked Flow Parameter ($[kg/s*K^{.5}]/[m^2*Pa]$)	0.01066	0.03415
Gas Constant ($J/[kg*K]$)	4124.18	376.03
Ratio of Specific Heats	1.4	1.272
Constant Pressure Specific Heat ($J/[kg*K]$)	14434.63	1758.46
Liquid Density (kg/m^3)	65.147	--
Thermal Time Constant (sec)	0.0005	0.0005

3.1.3 Turbopump Assembly

3.1.3.1 Pump Performance Maps

The coolant pump performance is based on similarity maps which define the normalized pump pressure rise and normalized shaft power as a function of normalized pump flow as described in paragraph 2.3.2.2. Figure 3.2 shows the performance maps used for the nominal engine cycle model [G-1]. The design pump efficiency is assumed to be 75%.

Figure 3.2 Pump Performance Maps

30
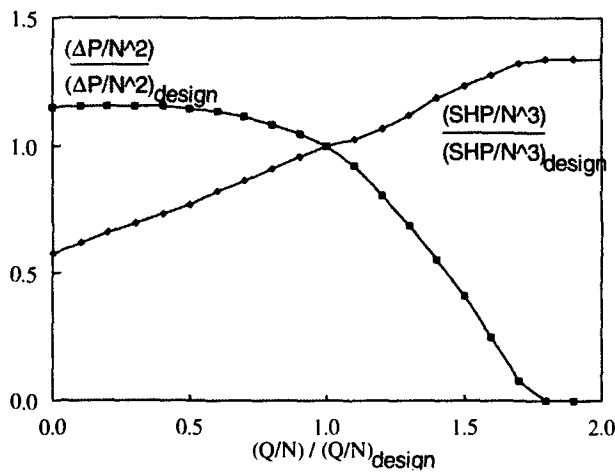
3.1.3.2 Turbine Performance

The turbine performance is determined as described in paragraph 2.3.2.2. Figure 3.3 shows the modeled turbine efficiency as a function of the normalized spouting ratio [G-1]. The design turbine efficiency is 45%.

Figure 3.3 Turbine Efficiency Map
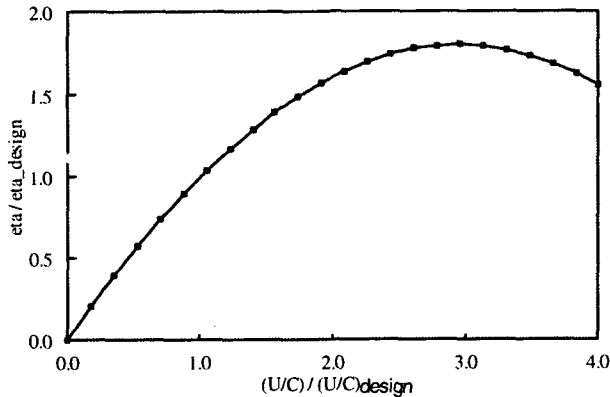
3.1.3.3 TPA Size

The TPA size is extrapolated from a high temperature turbopump assembly designed by Garrett Fluid Systems Division [O-1]. Only a single turbine stage is modeled, with a diameter of 0.18 m. The design TPA speed is 55600 rpm. The mass of the rotating portions of the TPA is estimated to be 10 kg. Based on this mass, and assuming that the radius of gyration is half the turbine radius, the TPA polar moment of inertia was estimated to be 0.010125 $kg*m^2$. The system performance is relatively sensitive to the assumed value of the TPA inertia since this value determines how much energy is required to accelerate the TPA to its design speed. This effect will be quantified and discussed in more detail in section 4.3.1.

3.1.4 Engine Design Balance

3.1.4.1 Coolant Flow Rates

In order to achieve the desired steady-state design conditions, the engine system flow rates must be balanced to provide the proper driving flow to the turbine. There are three

31

conditions which must be satisfied at the design conditions to achieve the proper engine balance: (1) the required pumping power must equal the turbine power produced; (2) the hot bleed flow and cold bypass flow must be balanced to provide the desired turbine inlet temperature; and (3) the total pump flow must equal the flow through the reactor and the cold bypass flow. These conditions can be expressed as follows:

1) $\dot{m}_p \times \dfrac{\Delta P}{\rho} \times \dfrac{1}{\eta_p} = \dot{m}_t \times c_p \times \eta_t \times T_{in} \times \left(1 - PR^{\frac{1-\gamma}{\gamma}}\right)$

2) $\dot{m}_t \times T_{in} = \dot{m}_h \times T_h + \dot{m}_c \times T_c$

3) $\dot{m}_p = \dot{m}_r + \dot{m}_c$

The pump pressure rise, reactor flow rate, and hot bleed flow temperature are calculated based on the reactor steady-state design as described in section 3.2.4 below. The fluid properties, TPA efficiencies, turbine pressure ratio, and the cold flow and turbine inlet temperatures have been defined. The above equations can therefore be solved simultaneously to find the design coolant flow rates. Table 3.3 summarizes the calculated flow rates for each portion of the engine system.

Table 3.3 Design Point Coolant Flow Rates

Location	Flow Rate (kg/s)
Pump	9.86802
Turbine	0.253095
Reactor	9.766
Cold Bypass	0.10203
Hot Bleed	0.151065
Main Nozzle	9.61492

3.1.4.2 Flow Area Sizing

The design point flow areas for the flow restricting elements in the engine model are calculated based on the design mass flow rate through the element and the design

32

pressure levels at the inlet and outlet (inlet only for choked flow elements) of the element. Table 3.4 summarizes the calculated flow areas for the engine model.

Table 3.4 Element Design Flow Areas

Element	Flow Area (m^2)
Pump Discharge Valve	1.9797e-3
Turbine Inlet	1.6930e-4
Turbine Exhaust Nozzle	2.2101e-3
Temperature Control Valve	1.1148e-5
Speed Control Valve	2.8248e-4

3.2 Reactor System

3.2.1 General Properties

The nuclear reactor model for the engine system is based on a representative particle bed reactor design. Since no complete PBR design has yet been published, the model used here is extrapolated from preliminary designs and the author's knowledge of particle bed reactor engines. The basic PBR design chosen is a 500 *MW* core consisting of 19 fuel elements. The elements are arranged in an hexagonal pattern with a center element surrounded by two rings of 6 and 12 elements, respectively. The fuel elements are embedded in a beryllium moderator and contained within a carbon-carbon composite pressure vessel. The SAFSIM reactor model also includes the main nozzle and the hot bleed valve.

3.2.2 Reactor Structure

3.2.2.1 Overview

For simplicity, only one of the 19 fuel elements and its associated coolant passages are modeled using the SAFSIM program. The reactor flow rate and the main nozzle and

bleed valve flow areas are scaled by 1/19 to account for the fact that only a single element is modeled. When the reactor model is linked to the remainder of the engine system model, the flow rates calculated by SAFSIM are rescaled to the full reactor size to properly couple the solutions. The reactor model is described in cylindrical coordinates and assumes axial symmetry. A schematic diagram of the single fuel element reactor model is shown in Figure 3.4. The hydrogen coolant enters the top of the reactor and then flows downward cooling the pressure vessel. The flow then turns and flows upward through a coolant passage in the moderator. The flow next cools the top axial reflector and enters the top of the inlet plenum. The hydrogen is then distributed axially and flows radially through the cold frit, fuel bed, and hot frit. The hydrogen then enters the exit plenum and turns to flow into the chamber region. The majority of the flow is exhausted through the main nozzle while a small portion is bled off through the bleed valve to run the turbine.

Figure 3.4 Single Element Reactor Model Schematic

34
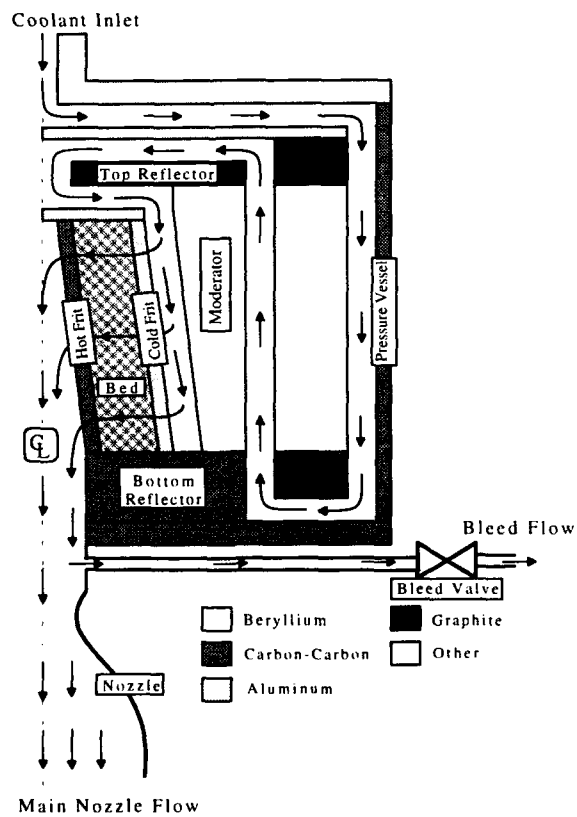
The SAFSIM reactor model contains 59 fluid mechanics finite elements connected at 58 nodes; the fuel element portion of the model includes 3 axial levels and 7 radial rings--1 for each frit and 5 for the fuel bed. Figure 3.5 shows the finite element diagram for the model. The reactor inlet pressure and temperature boundary conditions are imposed at node 1 which corresponds to the pump discharge plenum. The reactor outlet pressure boundary condition is imposed at node 58 which represents the bleed mixer. The choked flow element which models the main nozzle provides the final boundary condition for the SAFSIM portion of the model. The parameters which are used in the NTPSIM portion of the solution are the total reactor flow rate (measured at element 1), the bleed flow rate (element 59), and the bleed flow temperature (node 58).

Figure 3.5 Reactor Finite Element Diagram
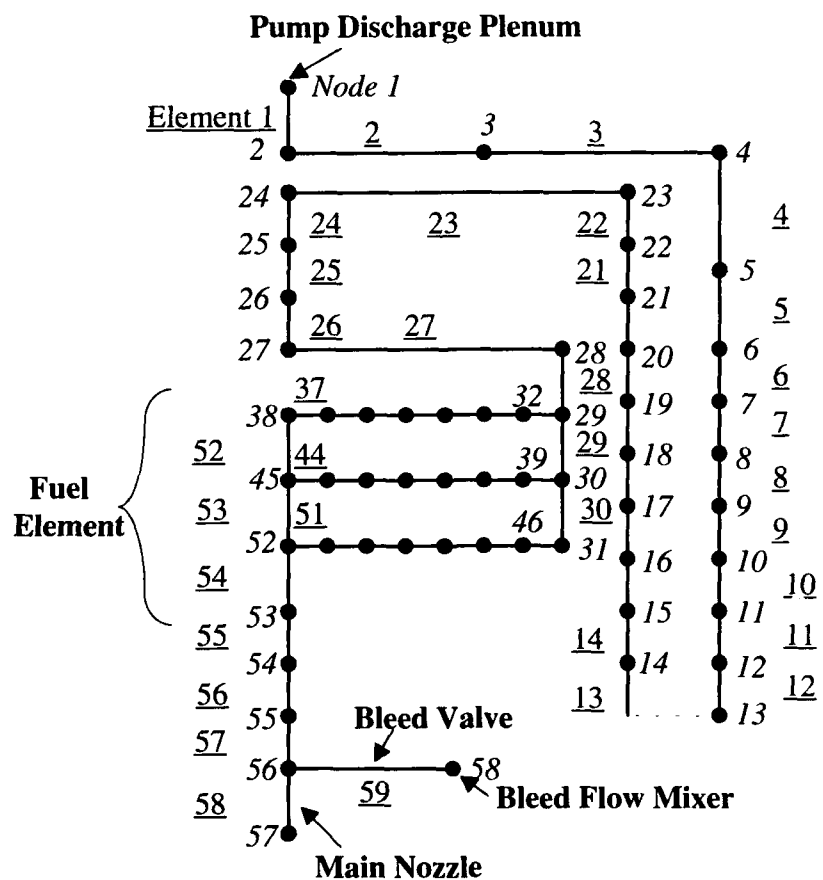
Figure 3.6 Fuel Element Design
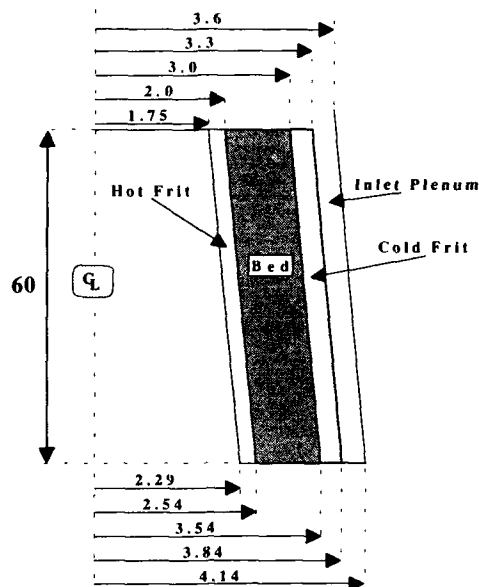
Notes: (1) all dimensions in cm
(2) radial dimensions drawn
approximately to scale

3.2.2.2 Fuel Element

The fuel element consists of the cold frit, fuel bed, and hot frit. Figure 3.6 shows the fuel element design including appropriate dimensions. The overall element size was chosen to achieve a 25.2 GW/m^3 bed averaged power density, which, for a 37% bed porosity, corresponds to a 40 GW/m^3 fuel volume power density. This power density was chosen based on preliminary PBR engine designs [L-3]. The fuel length and taper was chosen to ensure outlet plenum velocities less than about Mach 0.2. The bed pressure drop is calculated using the Ergun correlation and the heat transfer is modeled using the Achenbach correlation. The fuel particles are assumed to have a diameter of 500 μ. The bed porosity for the innermost and outermost rings was modeled as 37.8% and 37.2%, respectively, rather than the 37% used for the middle three rings, to account for increased voidage next to the frits. The cold frit is modeled using aluminum with a 35% porosity. The pressure drop is calculated using the Ergun correlation for the friction factor plus fixed loss coefficients to simulate the engineered pressure drop of the cold frit design.

36

The loss coefficients are varied over the three axial levels to achieve relatively uniform bed outlet temperatures. The hot frit is modeled as carbon-carbon; the pressure drop is calculated using a friction factor based on an equivalent diameter of 250 μ.

3.2.2.3 Moderator and Other Structures

The moderator model includes the approximate volume of beryllium associated with each of the 19 fuel elements for a centerline-to-centerline pitch of 11 cm. The moderator is cooled by hydrogen flow between the elements and in the fuel element inlet plenum. Other structures modeled in the reactor core include the carbon-carbon pressure vessel and the top and bottom graphite axial reflectors. Each of these structures is cooled by hydrogen flow.

3.2.3 Reactor Kinetics

3.2.3.1 Power Distribution

The reactor thermal power is assumed to be deposited in the fuel element as well as the moderator, axial reflectors, and pressure vessel. Table 3.5 shows the percentage of power deposited in each structure.

Table 3.5 Power Deposition in Core

Structure	Percent Power
Fuel Element	95.0
Moderator	3.5
Reflectors	0.5
Pressure Vessel	1.0

The heat generation in the fuel element has an exponential radial distribution as shown in Figure 3.7 [D-3]; there is no axial power variation modeled. The reflectors, moderator, and pressure vessel have axial power distributions as shown in Figure 3.8 [D-3]; no radial distribution is modeled. The bottom reflector power distribution is the mirror image of

37

the top reflector power distribution. The power profiles are modeled based on an average
fuel assembly.

Figure 3.7 Fuel Element Power Distribution
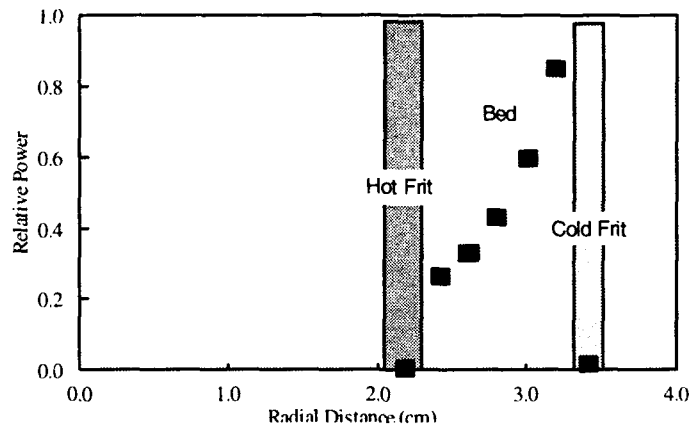
Figure 3.8 Axial Power Distributions in Core
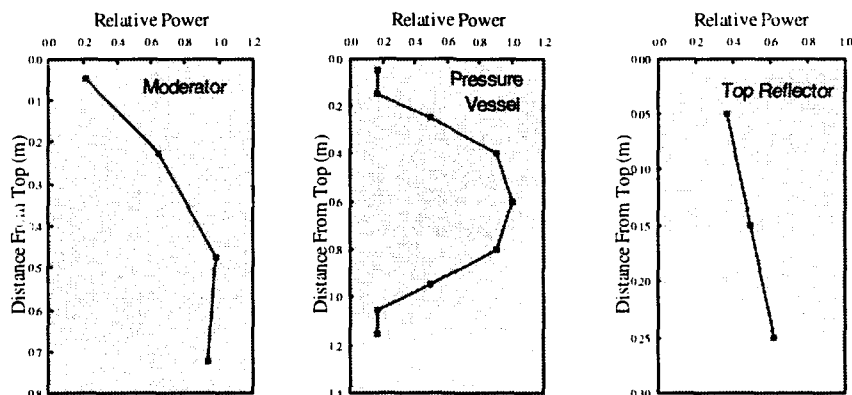
3.2.3.2 Point-Kinetics Parameters

The reactor dynamics for the PBR model are calculated using point-kinetics. The prompt
neutron lifetime is $33.3 \cdot 10^{-6}$ sec and the effective delayed neutron fraction is 0.0079 based
on measurements conducted by Ball, et. al. [B-1]. The delayed neutron fraction is
divided into 15 delayed neutron groups, including 9 photoneutron groups due to the

38

beryllium moderator. Table 3.6 summarizes the effective neutron fractions, β_i, and the effective decay constants, λ_i, for each group.

Table 3.6 Delayed Neutron Group Parameters

β_i	λ_i (sec)	β_i	λ_i (sec)
0.000256	0.0124	$3.0862 \cdot 10^{-6}$	$1.59 \cdot 10^{-5}$
0.00169	0.0305	$3.7984 \cdot 10^{-5}$	$6.20 \cdot 10^{-5}$
0.001513	0.111	$4.2732 \cdot 10^{-6}$	0.000267
0.003049	0.301	$4.3681 \cdot 10^{-5}$	0.000742
0.000888	1.14	$2.1960 \cdot 10^{-5}$	0.0036
0.00325	3.01	$4.3444 \cdot 10^{-5}$	0.00885
$6.7659 \cdot 10^{-7}$	$6.24 \cdot 10^{-7}$	$2.4571 \cdot 10^{-5}$	0.0226
$4.5106 \cdot 10^{-7}$	$2.48 \cdot 10^{-6}$		

3.2.3.3 Decay Heat Groups

Although the SAFSIM program includes the capability to model fission product decay heat generation, no decay heat groups are modeled. This is due to the very short time frame associated with the reactor startup. As will be shown in Chapter 4, the time scale for system startup is on the order of 10 sec, which does not allow enough time for significant buildup of decay heat precursors.

3.2.3.4 Reactivity Feedback

The reactor model includes the effects of six reactivity feedback terms. These are: doppler effect ($\Delta\rho_F$) and bed expansion ($\Delta\rho_{BE}$) based on the average fuel temperature; hot frit expansion ($\Delta\rho_{HF}$) based on the average hot frit temperature; coolant density ($\Delta\rho_{IP}$ and $\Delta\rho_{OP}$) based on the average inlet plenum and outlet plenum coolant densities,

39

respectively; and moderator temperature ($\Delta\rho_M$) based on the average moderator temperature. Table 3.7 shows the equations used for each feedback term [D-2].

Table 3.7 Reactivity Feedback Terms

$$\Delta\rho_F = -2.7 \cdot 10^{-5} \times \frac{\Delta T_{fuel}}{\sqrt{T_{fuel}}}$$

$$\Delta\rho_{BE} = 2.24 \cdot 10^{-7} \times \Delta T_{fuel}$$

$$\Delta\rho_{HF} = 7.0 \cdot 10^{-8} \times \Delta T_{HF}$$

$$\Delta\rho_{IP} = 1.204 \cdot 10^{-3} \times \Delta d_{IP}$$

$$\Delta\rho_{OP} = 7.0 \cdot 10^{-4} \times \Delta d_{OP}$$

$$\Delta\rho_M = (-9.76 \cdot 10^{-5} + 4.4398 \cdot 10^{-8} \times T_M + \ldots$$
$$0.040958 \times \frac{1}{T_M} + 1.17507 \times \frac{1}{T_M^2}) \times \Delta T_M$$

3.2.3.5 Control Drums

The mechanisms used to control the reactor reactivity are rotating control drums located in the reflector region. As the drums rotate, they expose varying amounts of a neutron poison material which increases neutron absorption in the reflector region and reduces the core reactivity. The drum reactivity worth has a span of 0.0470 or $5.95 with a sinusoidal variation as shown in Figure 3.9. The initial critical state is assumed to occur with the control drums at 90° at an idling power of 5.0 kW. The drum rotation rate is limited to 180° per second.

3.2.4 Steady-State Design

3.2.4.1 Mass Flow and Inlet Pressure

The design point reactor coolant flow rate was determined using the SAFSIM program by imposing a mass flow and temperature boundary condition at the reactor inlet and a pressure boundary condition at the reactor chamber. The inlet temperature was set to 52.91 K and the chamber pressure was set to 7.0 MPa. The mass flow rate was then varied until a chamber temperature within a few degrees of 3000 K was achieved. The

coolant flow rate was found to be 0.514 *kg/sec* for the single element modeled; this value was multiplied by 19 fuel elements to give the 9.766 *kg/sec* flow rate shown in Table 3.3. The required inlet pressure to achieve this flow rate, as calculated by SAFSIM, was 7.8933 *MPa*.

Figure 3.9 Control Drum Worth
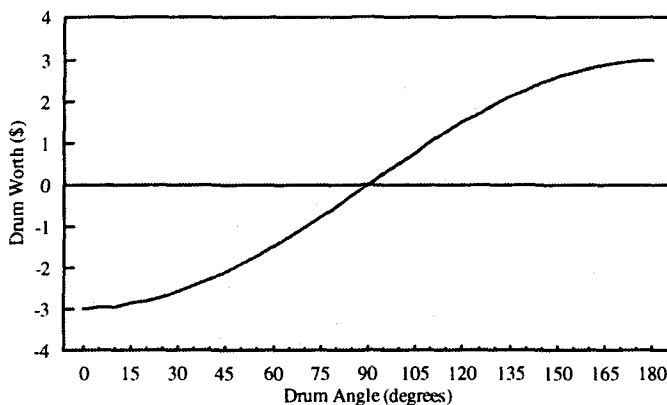
3.2.4.2 Main Nozzle and Bleed Valve

The main nozzle was sized by modeling only the chamber and nozzle in SAFSIM. The chamber pressure and temperature were imposed as boundary conditions, and the flow area of the nozzle was varied until the required mass flow rate (9.61492 / 19 = 0.50605 *kg/sec*) was achieved. The bleed valve was sized by modeling only the chamber, nozzle and bleed valve. The reactor pressure and temperature, and the nozzle and bleed valve flow rates were imposed as boundary conditions. The bleed valve flow area was then varied until the desired bleed mixer pressure (6.454 *MPa*) was achieved. The temperature of the bleed flow entering the mixer was found to be 2980 *K*.

3.3 Engine Performance Summary

The engine thrust is calculated assuming a main nozzle expansion ratio of 50:1 and a turbine exhaust nozzle expansion ratio of 10:1. The thrust, based on isentropic nozzle flow, is 92.94 *kN* for the main nozzle and 1.38 *kN* for the turbine exhaust nozzle. The

main nozzle specific impulse is 985 *sec* and the overall system I_{SP} is 974 *sec*. Table 3.8 provides a summary of the engine system design parameters.

Table 3.8 Engine Design Parameters

Parameter	Value
Total Thrust	94.32 *kN*
System Specific Impulse	974 *sec*
Chamber Pressure	7.0 *MPa*
Chamber Temperature	3000 *K*
Reactor Idle Power	5.0 *kW*
Reactor Rated Power	500 *MW*
Fuel Volume Power Density	40 *GW/m³*
Turbopump Assembly Speed	55600 *rpm*
Turbine Inlet Temperature	1800 *K*

Chapter 4 Startup Controller Development and Analysis

4.1 Control Framework

4.1.1 Startup Strategy Goal

The goal of the startup control strategy is to bring the particle bed reactor engine system from an idle-power/zero-flow configuration to full-power/full-flow operation as quickly as possible while maintaining coolant flow through the PBR fuel elements in the stable operating regime. The full-power/full-flow operating conditions were shown in Table 3.8. Table 4.1 summarizes the idle-power/zero-flow engine configuration.

Table 4.1 Idle-Power/Zero-Flow Parameters

Parameter	Value
Reactor Power	5.0 kW
System Pressure	0.1 MPa
Fluid Temperature	300 K
Material Temperature	300 K
Turbopump Assembly Speed	0.01 rpm

4.1.2 Overall Engine Control

The engine system startup controller examined in this thesis forms only a small portion of the overall engine controller required for operation of a nuclear thermal propulsion rocket engine. A complete engine controller must incorporate strategies to address startup as well as full power, throttling, shutdown, and cooldown operation modes. In addition, for each operation mode, the controller must address issues such as:

a) stability and performance robustness in the presence of modeling errors, external disturbances, and sensor noise;

43

b) fault tolerance and reliability in the presence of sensor failures, actuator failures, and engine faults;

c) reactor safety including the ability to shutdown and remove decay heat during all phases of operation.

High level supervisory control will be needed to oversee these functions. A possible framework for the required elements of a complete NTP engine controller has been described by Parlos [P-1].

4.1.3 General Startup Framework

The control architecture presented in this thesis applies only to the startup phase of engine operation. Based on preliminary investigations of the PBR startup behavior using an NTPSIM engine model, it was decided that a combination of open-loop scheduling and several independent single-input single-output control loops would provide the best general framework for continuing investigation. The startup strategies from the NERVA program [see for example, N-1], which often included multivariable control using linearized systems models, were not considered to provide a desirable baseline since they utilized transients on the order of several minutes for startup. One of the benefits of the PBR engine is the ability to reach design conditions much faster than NERVA or NERVA-derivative engines. Multivariable control was not considered for the startup phase due to the very fast transients and the highly nonlinear system response over the range of operating conditions encountered during startup. Very little theory exists for nonlinear multivariable control, requiring linearization of the system model for application of general multivariable control theory; these restrictions make multivariable control undesirable during system startup. However, during steady-state operation where linearization of the system model is more feasible, a multivariable control strategy will probably be desirable.

44

4.1.4 Neutronic Power Control

4.1.4.1 General Requirements

The most unique feature of nuclear rocket engine control is the need to control the reactor neutronic power. The reactor power must be coordinated with the hydrogen coolant flow through the reactor in order to maintain reactor material temperatures below the design safety limits. Therefore, closed-loop control of reactor power with the demanded power being a function of the measured flow rate was chosen to effect reactor power control. This method was chosen for two reasons:

a) since the system flow time scale is much slower than the reactor power time scale, controlling flow rate based on reactor power would not be feasible during startup;

b) this strategy would provide the best safety (before supervisory control can be effected) in case of a lower than expected coolant flow rate or even a loss of coolant flow.

4.1.4.2 Implementation

The MIT/SNL Minimum Time Control Law, developed by the Massachusetts Institute of Technology and Sandia National Laboratories, was chosen to control reactor power; this law has been extensively tested and has been shown to accurately and quickly maneuver reactor power over large operating regimes [B-3]. The application of the MIT/SNL control law for this study, though, is somewhat different from previous applications. Experiments on the MITRII research reactor and SNL Annular Core Research Reactor have controlled reactor power using a predetermined power profile. However, as described above, the demanded power for the engine system must be calculated on-line based on the measured coolant flow rate. The algorithms used are the same, except that the power projection interval which sets the number of control intervals to regain the desired power profile becomes the number of control intervals to achieve the currently desired power; no attempt is made to project the demanded power based on expected flow rates. The control law also includes a differential reactivity feedback term which must be calculated based on estimates of the feedback effects and measured core conditions. The

45

controller used in this study does not estimate the differential reactivity feedback. In effect, the derivative of the feedback reactivity is assumed to equal zero, which is equivalent to assuming that the core material temperatures and fluid properties do not change appreciably between control intervals. This assumption appears to be reasonable; in any case, the design of the MIT/SNL control law is such that the desired power should be achieved despite unmodeled feedback effects, though an initial undershoot or overshoot may be expected.

4.1.5 Base Line Strategy

4.1.5.1 General Description

The initial control strategy implemented for the PBR engine system model was designed to provide a base line reference case and establish the significance of the flow instability issue during startup. The base line strategy uses a very simple control scheme as described below.

4.1.5.2 Reactor Power Control

The base line coordination strategy for the reactor power as a function of coolant flow rate was to match the demanded reactor power linearly to the measured flow rate. That is, if the measured flow rate is X% of the design flow rate, the demanded power will be X% of the rated power. However, the demanded reactor frequency is not allowed to exceed 5.0 sec^{-1} in order to prevent the reactor from going prompt critical. This strategy was chosen to achieve high reactor outlet temperatures throughout the transient. The reactor control interval is 0.01 sec; the power projection interval is chosen to be 4 control intervals.

4.1.5.3 Flow Control

The flow control strategy for the base line case uses open-loop scheduling for all valves. The pump discharge valve is opened to its design point from 0.0 to 4.0 sec. The effective flow area is assumed to vary sinusoidally as the valve angle varies linearly. The bleed valve is maintained at its design point flow area throughout the transient. The turbine

46

temperature control valve and speed control valve are initially closed but are opened to their design point conditions within about 0.2 *sec*. The flow control interval is 0.1 *sec*. The base line startup strategy does not utilize an external starter system.

4.1.5.4 Results

The engine performance for the base line control strategy is shown in Figures 4.1 to 4.4; The data in Figures 4.1 to 4.3 are normalized to the design operating conditions for ease in interpreting the results. Figure 4.1 shows the successful coordination of the reactor power to the coolant flow rate. The initial lag in reactor power is due to the limit on the maximum allowed reactor frequency. The importance of power/flow coordination is evident by the prevention of full reactor power when the coolant flow rate does not achieve the rated value; if full power had been demanded, the reactor coolant temperature might exceed design limits. Figure 4.2 shows the response of chamber pressure and chamber temperature. The chamber temperature increases quickly and reaches the design value in about 5 *sec* due to the effect of the linear power/flow coordination. The chamber pressure rises to within about 5% of its design value in approximately 7 *sec*. At this point, the pressure very slowly converges towards the design operating point. The reason for the slow convergence appears to be due primarily to the time required for the engine system, particularly the outer moderator and pressure vessel temperatures, to reach equilibrium. As the cold hydrogen enters the reactor, it slowly cools these components. This effect is countered somewhat by heat generation within the structures, and it takes a long time for the equilibrium temperatures—which were used in the steady-state design of section 3.2.4—to be reached. This small deviation from the equilibrium state affects the pressure drop through the core such that the design plant balance is not achieved until the equilibrium temperature is reached. Figure 4.3 shows the response of the turbopump assembly; the acceleration is initially quite small due to the low energy flow available to drive the turbine. The flow stability through the fuel element is analyzed by plotting the element temperature rise ratio, Φ, as a function of the superficial Reynolds number at the bed inlet over the course of the transient. The values are calculated for the middle axial level in the SAFSIM model. The bed inlet is considered to be the node between the cold

47

frit and the first fuel bed ring; the bed outlet is considered to be the node between the last fuel bed ring and the hot frit. Figure 4.4 shows that during the course of the transient the PBR fuel element operates very close to the flow instability region as it is currently understood. These results indicate that the issue of flow instability is in fact a concern during startup of a particle bed nuclear rocket engine.

Figure 4.1 Reactor Power and Coolant Flow for Base Line Strategy
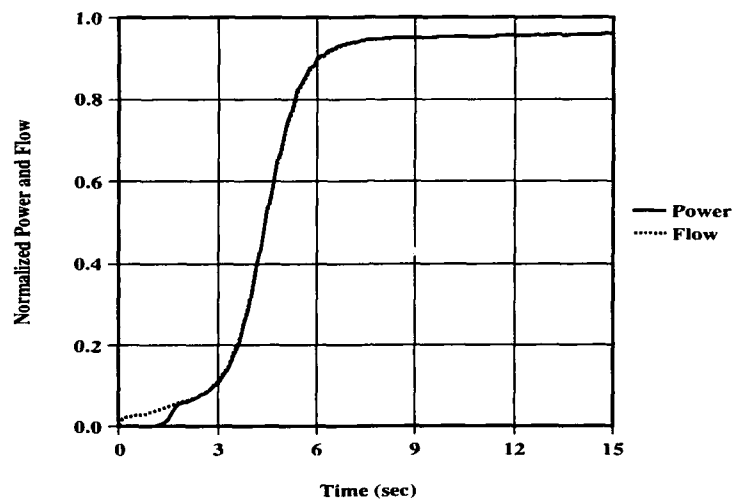
Figure 4.2 Chamber Conditions for Base Line Strategy
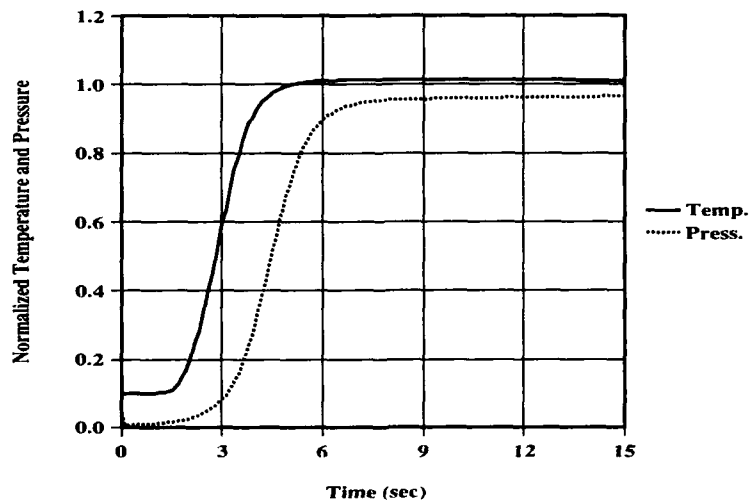
Figure 4.3 TPA Speed for Base Line Strategy
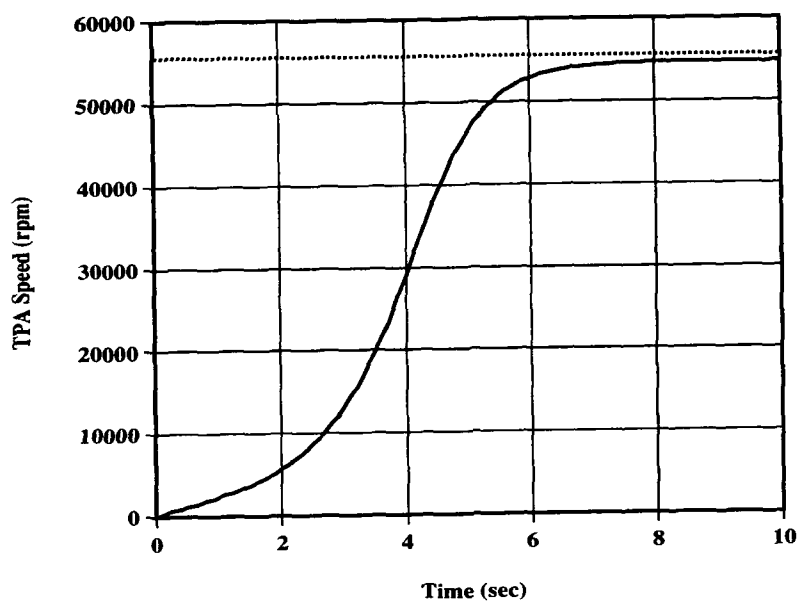
Figure 4.4 Stability Map for Base Line Strategy
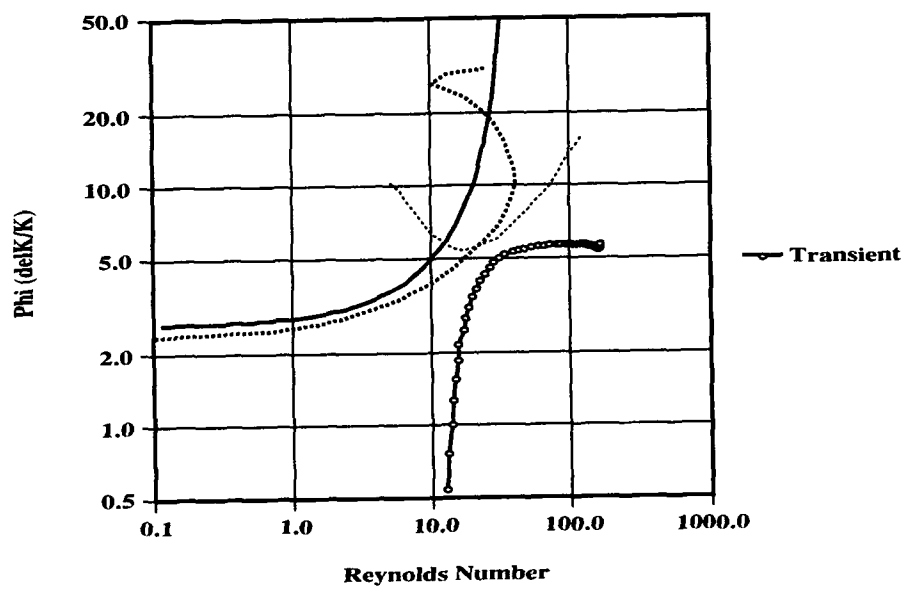
4.2 Strategy Development and Analysis

4.2.1 Focus of Improvements

By examining the base line startup strategy, there appear to be three major areas where improvement of the engine startup controller should be focused:

a) movement of the transient away from the flow instability boundary;

b) improving convergence to the design chamber conditions;

c) increasing the startup response speed.

Some elements of the startup strategy which are considered to achieve these improvements are the coordinated control of reactor power and coolant flow, turbine coolant temperature and flow control, and use of an external starter system.

4.2.2 Power/Flow Coordination

4.2.2.1 Objective

In order to move the transient away from the flow instability boundary, the coolant temperature at the element outlet must be reduced at the initial low flow rates, or the flow rate must be increased while outlet temperatures are low. The latter approach is difficult with a bootstrap start since the energy available to drive the turbine is controlled largely by the bleed flow temperature. Thus, in order to reduce the element outlet temperature, the coordination algorithm for reactor power as a function of reactor coolant flow rate was modified.

4.2.2.2 Implementation

The base line linear coordination algorithm for reactor power and flow was designed to give approximately uniform outlet temperatures for all flow rates. Therefore, to enhance flow stability, a cubic relation was chosen which reduces the demanded power at lower coolant flow rates. The coordination relation used is:

$$p = 7.18327 \cdot 10^{-6} \times w^3 + 5.37824 \cdot 10^{-3} \times w^2 + 0.390329 \times w + 2.5 \cdot 10^{-4}$$

where p is the percent of rated reactor power demanded and w is the percent of rated coolant flow measured. This relation is shown if Figure 4.5.

Figure 4.5 Cubic Power/Flow Coordination
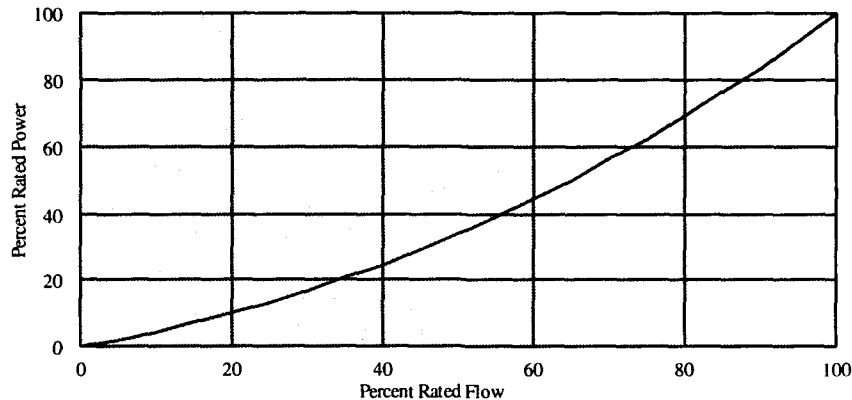
Figure 4.6 Stability Map with Cubic Power/Flow Coordination
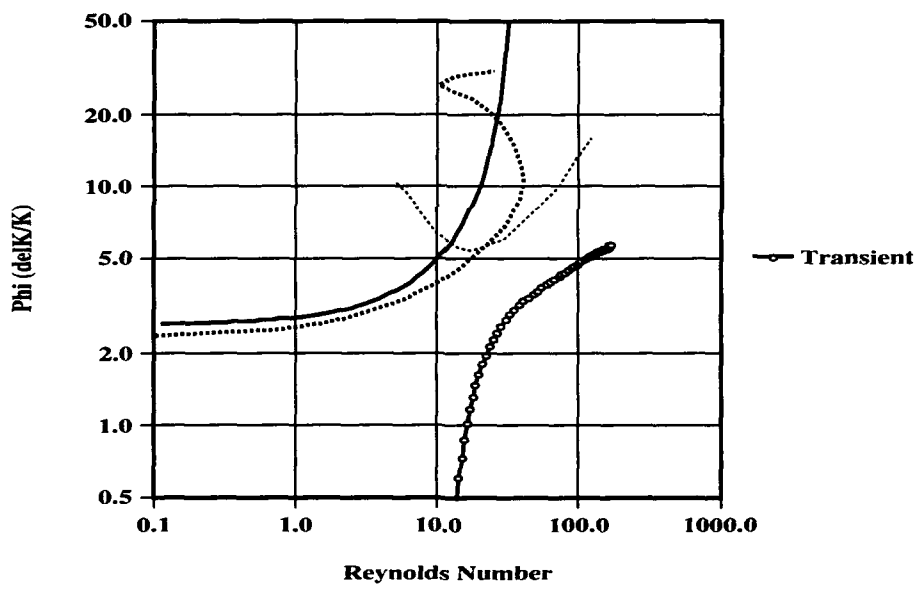
4.2.2.3 Results

The modification to the power/flow coordination algorithm, while maintaining all other control as in the base line strategy, had the expected effect of enhancing flow stability through the fuel element as shown in Figure 4.6. It can be seen that the transient progresses well away from the flow instability region, but reaches the same design operating point. Figure 4.7 shows the chamber conditions for this strategy. As a consequence of the reduced power, and thus chamber temperature, at lower flow rates,

51

there is less energy available at the turbine to accelerate the TPA. This results in a slower transient, with the system reaching within 5% of the design conditions in about 10 *sec* rather than 7 *sec*. The effect of the power/flow coordination can also be seen in the reduced lag between the chamber pressure and the chamber temperature.

Figure 4.7 Chamber Conditions with Cubic Power/Flow Coordination
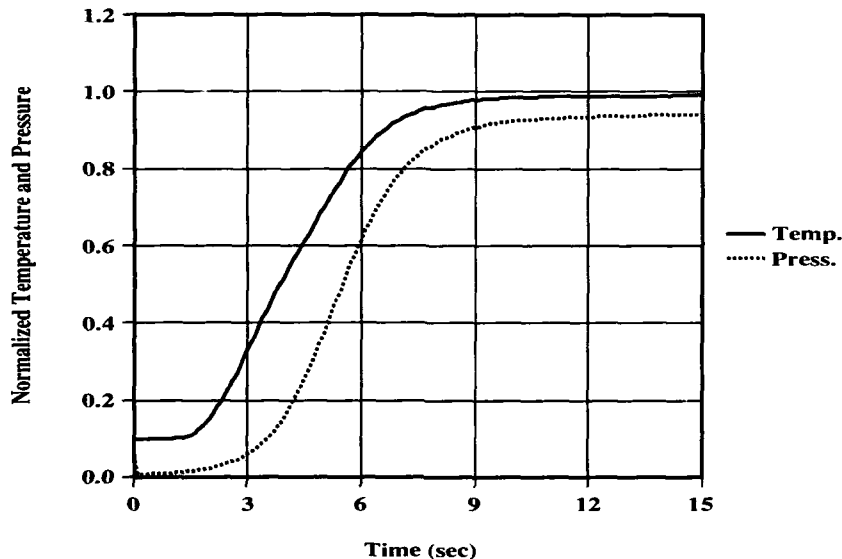
4.2.3 Turbine Flow Control

4.2.3.1 Objective

The next strategy development was to control the amount of hydrogen flow reaching the turbine by adjusting the turbine speed control valve (SCV). This development had two objectives: (1) to increase system response speed; and (2) to improve convergence to the design chamber pressure.

4.2.3.2 Implementation

To increase system response speed, the turbine SCV was initially opened beyond the design point position, thus increasing the effective flow area and allowing more flow to reach the turbine during the initial phase of startup. It was expected that this added flow

52

would help accelerate the TPA and thus increase the speed of the system response. In order to improve convergence to the design chamber pressure, a closed-loop control law was implemented to control the SCV flow area based on the measured chamber pressure. The controller initially demands a flow area greater than the design value, and then reduces the flow area to the design point as the chamber pressure approaches its design condition. In this manner, more flow is available to accelerate the TPA when the chamber pressure is low. Then, as the design pressure is reached, the SCV is returned to its design position to achieve the proper plant balance. Based on observation of the system response to various simple control laws, a relation for the demanded SCV flow area as a function of the measured chamber pressure was formulated. This relation is shown in Figure 4.8.

Figure 4.8 Control Law for SCV Area vs. Chamber Pressure
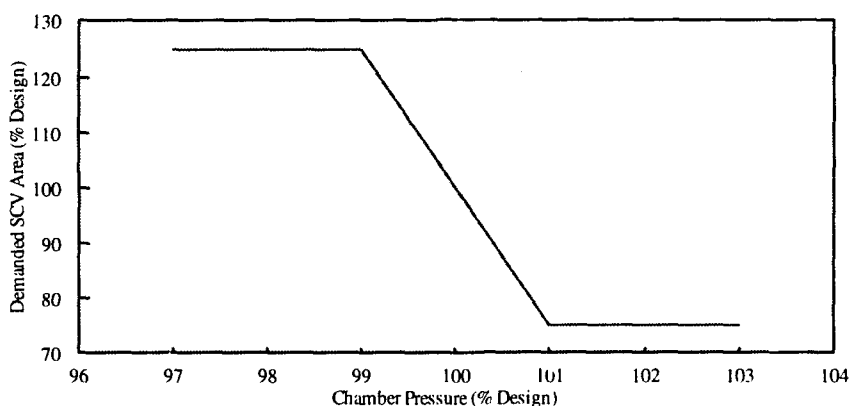
4.2.3.3 Results

The SCV control algorithm was implemented while maintaining the cubic power/flow coordination and the base line control for all other valves. The effect of this strategy development on the reactor chamber conditions is shown in Figure 4.9. It can be seen that the closed-loop chamber pressure control effectively drives the system to the desired design conditions. However, the system response speed is only slightly affected if measured in terms of the time required to achieve 90% of the design condition. The turbine SCV flow area is shown in Figure 4.10. It can be seen that the controller

53

effectively reduced the SCV flow area once the design chamber pressure was approached. However, the valve position exhibits a large degree of oscillation due to the rather simplistic formulation of the control law. There was no appreciable change to the transient flow stability as a result of incorporating the SCV control law.

Figure 4.9 Chamber Conditions with SCV Control
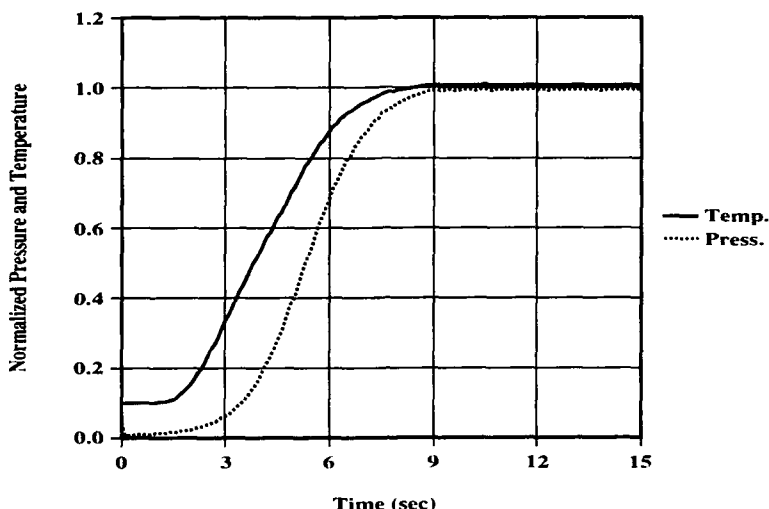
It should be noted that the SCV control law requires fairly accurate measurements of the chamber pressure, which may be difficult to achieve for an actual engine system. In addition, there will be a need to establish a dead-band around the design chamber condition to prevent rapid oscillation of the SCV around its design position. It is also possible that the overall engine controller will switch from the startup mode control to the steady-state operation control when the engine approaches within 5-10% of its design operating condition. Therefore, the control law described above is not directly applicable to actual control of an NTP rocket engine, but the results demonstrate three important aspects of the startup strategy:

a) closed-loop control of chamber pressure using the SCV can improve convergence to the design operating conditions;

54

b) increasing the SCV area during the initial phases of startup does not substantially affect system response speed;

c) controlling the SCV area does not appreciably impact flow stability during the startup.

Figure 4.10 SCV Flow Area with SCV Control
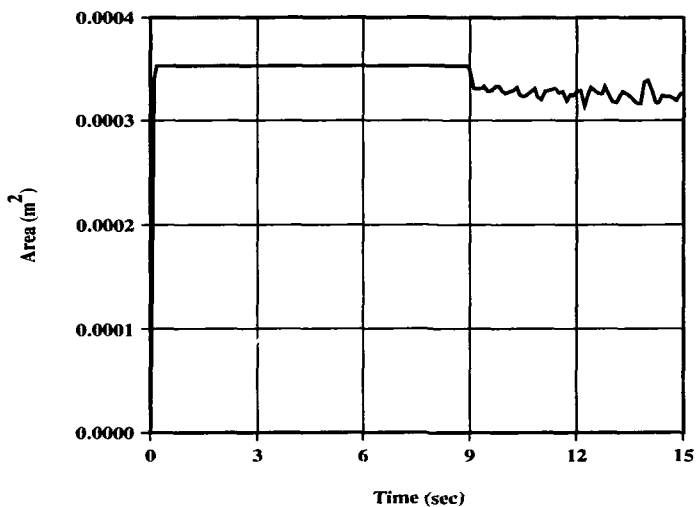
4.2.4 Turbine Inlet Temperature Control

4.2.4.1 Objective

Figure 4.11 shows the relation between the turbine inlet temperature and the chamber temperature for the above strategy. The graph shows that the flow initially entering the turbine is significantly colder than the design operating temperature of 1800 K, even after the chamber temperature surpasses this value. Therefore, the next strategy development was to add turbine inlet temperature control via the temperature control valve (TCV), thus adjusting the amount of cold flow mixed with the hot bleed flow. The objective of this step was to reduce the amount of cold flow--which has little available energy--that enters the turbine, thus conserving propellant and possibly increasing the system response speed.

Figure 4.11 Turbine Inlet Temperature without TCV Control
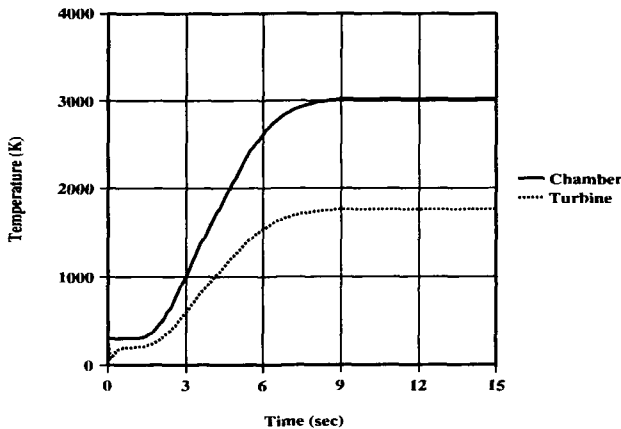
4.2.4.2 Implementation

The control of the turbine inlet temperature is achieved by adjusting the cold flow based on the measured hot bleed flow rate. The desired amount of cold flow is calculated from the measured bleed flow rate, bleed flow temperature, and cold flow temperature according to: $w_{cold} = \dfrac{w_{hot} \times (T_{hot} - 1800)}{1800 - T_{cold}}$ if the bleed flow temperature is above 1800 K; if the bleed temperature is below 1800 K no cold flow is allowed. The demanded flow area required to achieve the desired cold flow rate is calculated using the same orifice flow equations used by the NTPSIM program. This equation requires that the pump discharge plenum and bleed flow mixer pressures also be measured.

4.2.4.3 Results

The addition of the turbine temperature control law successfully regulated the turbine inlet temperature to 1800 K as shown in Figure 4.12. However, there was no appreciable impact on the system response speed; flow stability during the transient was also not affected. This appears to be due to the very low enthalpy of the cold fluid; since the enthalpy is low, its presence at the turbine does not significantly affect the total energy available to drive the TPA. Other effects, such as the power required to pump the extra amount of cold flow and the slightly altered flow conditions at the SCV do not appear to

be significant. Therefore, turbine temperature control can conserve a small amount of propellant, but does not appear to significantly affect the PBR engine system performance during startup. However, turbine temperature control will be needed to implement the next strategy development.

Figure 4.12 Turbine Inlet Temperature with TCV Control
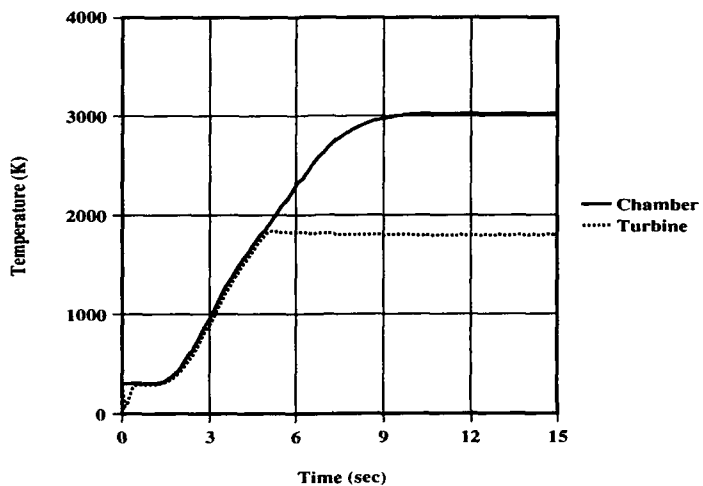
4.2.5 Bleed Flow Control

4.2.5.1 Objective

The goal of the next step in the startup strategy development was to decrease the system response time by increasing the initial energy delivered to the turbine. Since neither increasing the SCV area nor adding temperature control decrease system response time appreciably, a different method was required. The first alternative was to augment the hot bleed flow from the reactor chamber by increasing the bleed valve flow area beyond the design condition during the initial phase of startup.

4.2.5.2 Implementation

The bleed valve flow area was controlled based on the chamber pressure. The chamber pressure was not chosen so that it could be controlled, but rather because it provided a broad measure of the progress of the transient. The demanded bleed valve area as a function of the chamber pressure is shown in Figure 4.13. Temperature control via the TCV is used to maintain the turbine inlet temperature at 1800 K over the range of bleed flows encountered during the transient.

Figure 4.13 Demanded Bleed Valve Area vs. Chamber Pressure
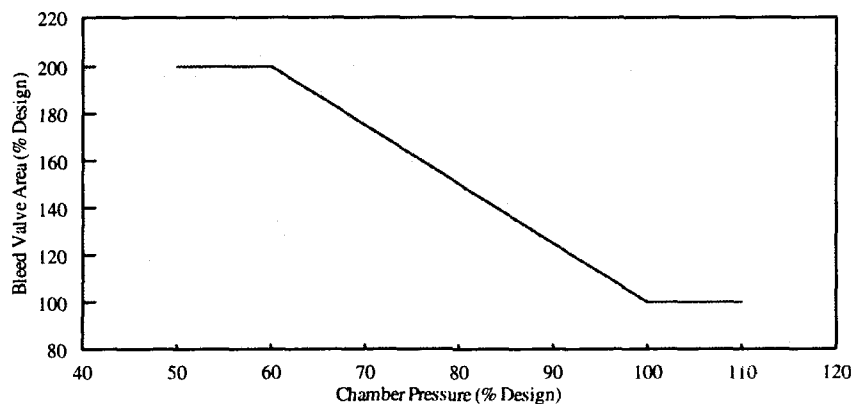
4.2.5.3 Results

This addition to the control strategy had the expected effect of making the system response more rapid, reaching design conditions in about 6.0 *sec* as shown in Figure 4.14. The transient flow stability, as seen in Figure 4.15, is not significantly different from the transient which used only the cubic power/flow coordination. This strategy, which includes the cubic power/flow coordination algorithm, closed-loop chamber pressure control via the SCV, turbine inlet temperature control via the TCV, and increased bleed flow via the BV, will be referred to as the "Fast Bootstrap Start." This startup control strategy meets the basic design objectives of reaching design conditions very quickly while maintaining operation of the PBR fuel element in the stable flow regime. Additional simulation results for the Fast Bootstrap Start are included in Appendix C.

Figure 4.14 Chamber Conditions for Fast Bootstrap Start
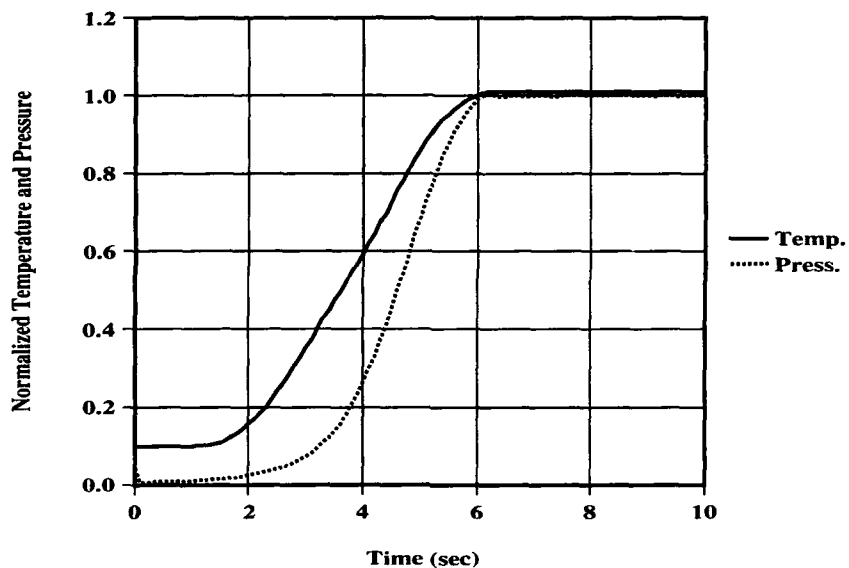
Figure 4.15 Stability Map for Fast Bootstrap Start
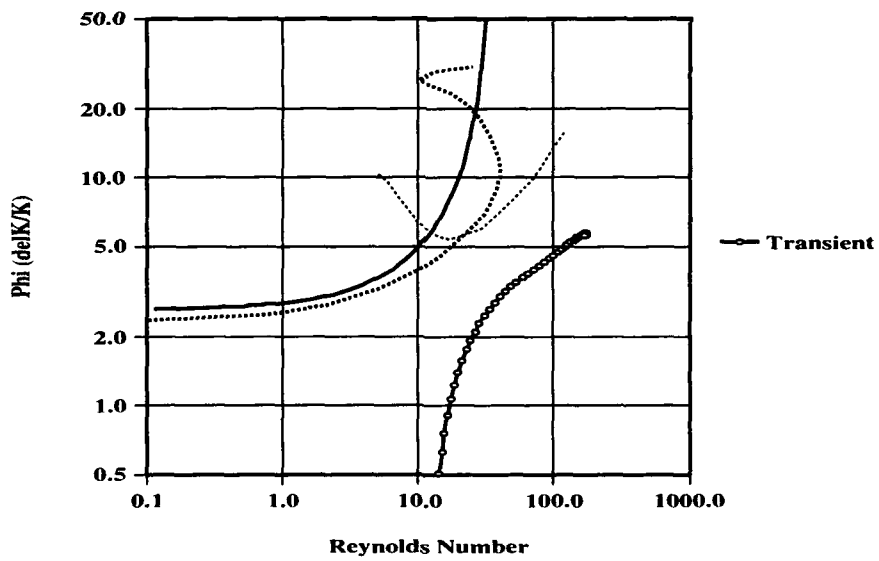
The results of the Fast Bootstrap Start provide important information about bootstrap startup strategies for a PBR engine system. The most significant finding related to the issue of flow instability during startup is that the coordination between the reactor power

and the coolant flow rate is the dominant factor which affects the location of the transient on the flow stability map. Other aspects of the engine controller can be implemented which significantly impact system performance, but these changes have almost no effect on the flow stability during the transient. Another finding is that the system response speed for a bootstrap start is controlled largely by the temperature and amount of hot bleed flow from the reactor chamber during the initial phase of startup. Since the temperature is likely to be controlled by the stability requirements as just described, the only viable means of increasing the response speed is to increase the initial bleed flow from the chamber. Finally, it was found that some form of control will be needed to ensure rapid convergence of the system to the design operating conditions. It is important to note that this requirement is due to the inherent nature of the system response as it approaches equilibrium. It will also be necessary to incorporate closed-loop control to account for model uncertainties, disturbances, sensor noise and other issues not addressed by the deterministic system model used in this study.

4.2.6 Starter System

4.2.6.1 Objective

In order to increase the speed of the system response beyond that achievable with a bootstrap start, a starter system was added to the engine system. The starter system chosen for the engine is a small solid rocket motor which exhausts its propellant into the turbine as described in section 3.1.2. The function of the starter system is to quickly accelerate the turbopump assembly before significant hot bleed flow is available from the reactor chamber, thus rapidly increasing the propellant flow.

4.2.6.2 Implementation

The primary design parameter for the starter system is the burn profile, including both the length of the burn and the propellant mass flow profile. A great deal is known about solid rocket motor combustion, and both of these factors can be readily tailored by proper design of the propellant grain. The burn profile was chosen by iterating the design until a desirable system response was achieved. The starter system chosen burns for 2.7 *sec* and

has a regressive burn as shown in Figure 4.16. The strategy used with the starter system includes the cubic power/flow coordination, closed-loop chamber pressure control via the SCV, and turbine temperature control via the TCV; the PDV is opened from 0-3.0 *sec* and the BV is maintained at its design position throughout the transient.

Figure 4.16 Starter Cartridge Burn Profile
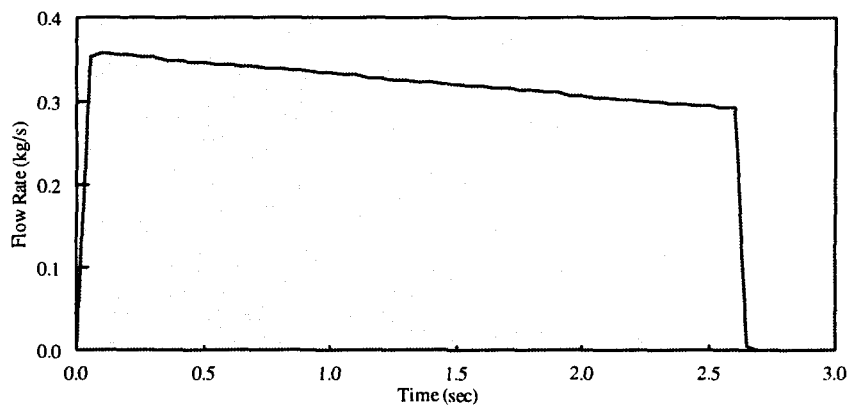
4.2.6.3 Results

The PBR engine performance using the starter system is shown in Figures 4.17 to 4.21. Figure 4.17 shows the dramatic effect on the TPA speed due to the ignition of the starter cartridge. The TPA is quickly accelerated to about 60% of the design speed, resulting in a rapid increase in propellant flow as seen in Figure 4.18. The TPA speed and flow then decrease slightly until the power rise catches up with the flow; at this point the power and flow rapidly increase, achieving the design conditions in only 2.8 *sec*. Figure 4.19 shows that the chamber pressure and temperature also reach the rated operating point in 2.8 *sec*. It is interesting to note that while there is a small overshoot in reactor power, there is no significant overshoot in chamber temperature. This is due to the small amount of additional energy represented by the power overshoot since its duration is very short. The rapid rise to the design conditions after the TPA decelerates slightly is due to the initiation of hot bleed flow from the chamber as is evident from Figure 4.20. There is no bleed flow initially since the chamber pressure is lower than the starter system exhaust pressure. It was found that the design of the starter motor is critical to ensuring the

61

proper coordination between the initiation of the bleed flow and the burnout of the starter system. If the system is not well designed, the TPA may decelerate substantially before bleed flow is initiated, thus eliminating the increased system speed gained by the TPA; or, if the starter system continues to burn too long after bleed flow is established, the system may severely overshoot the desired operating point. The effect of the starter system on the flow stability during the transient is quite profound, as seen in Figure 4.21. The stability is greatly enhanced since the starter system enables high coolant flow rates without the need for high coolant exit temperatures. Additional results from the simulation are shown in Appendix D.

Figure 4.17 TPA Speed with Starter System
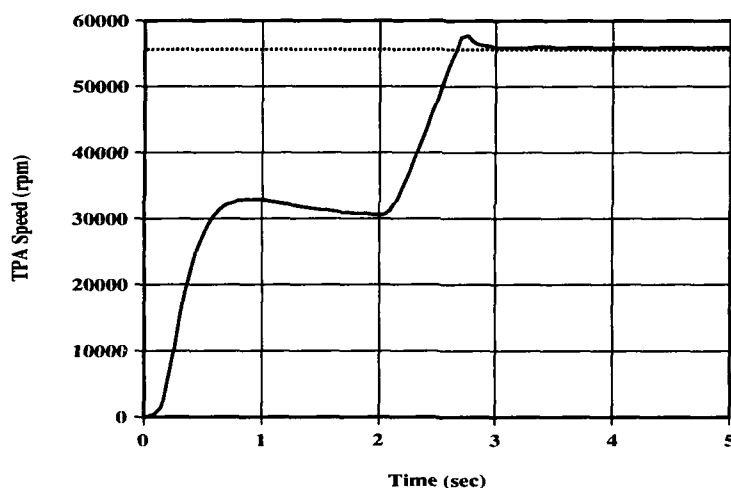
As with the Fast Bootstrap Start, the results of the Starter System Strategy provide important general information about startup strategies for a PBR rocket engine. First, the addition of a starter system enables the system to reach the design operating conditions very quickly. However, the starter system operating characteristics must be precisely designed to achieve a desirable system response. Since the solid rocket motor used for the system has no possible closed-loop control mechanism, the proper design of the system will require extensive modeling and testing of the starter system and the entire engine system to ensure proper operation. Second, the addition of a starter system can

significantly enhance the flow stability through the PBR fuel element during the startup. The importance of this aspect of the starter system performance will be more clear when the flow instability phenomena is better understood.

Figure 4.18 Reactor Power and Flow with Starter System
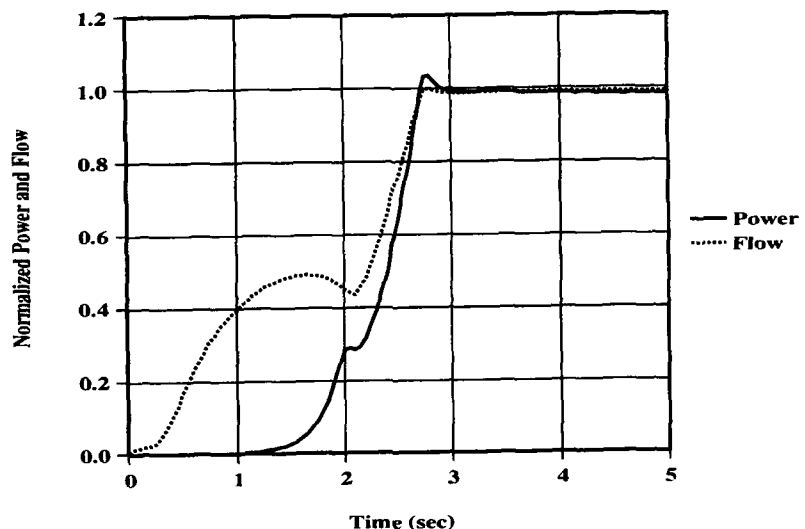
Figure 4.19 Chamber Conditions with Starter System
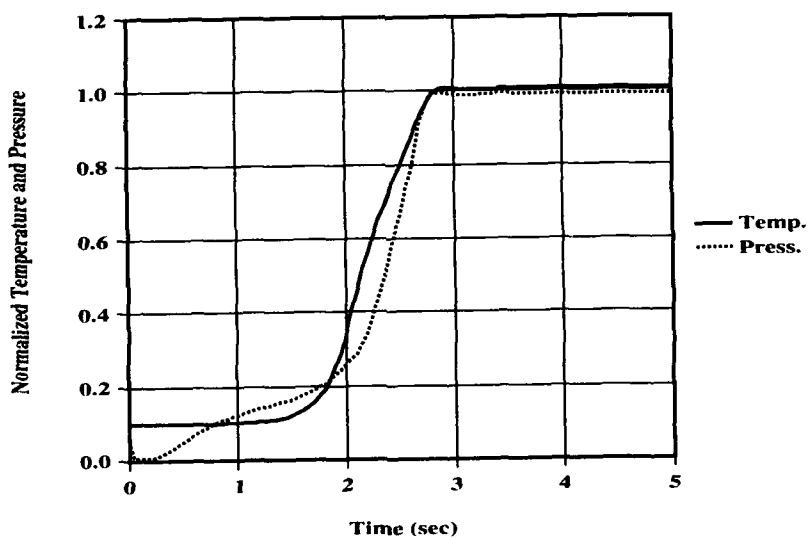
Figure 4.20 Turbine Flow with Starter System
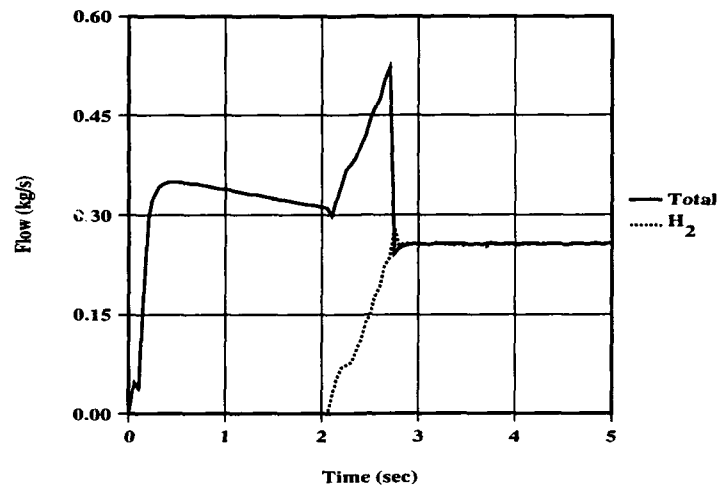
Figure 4.21 Stability Map with Starter System
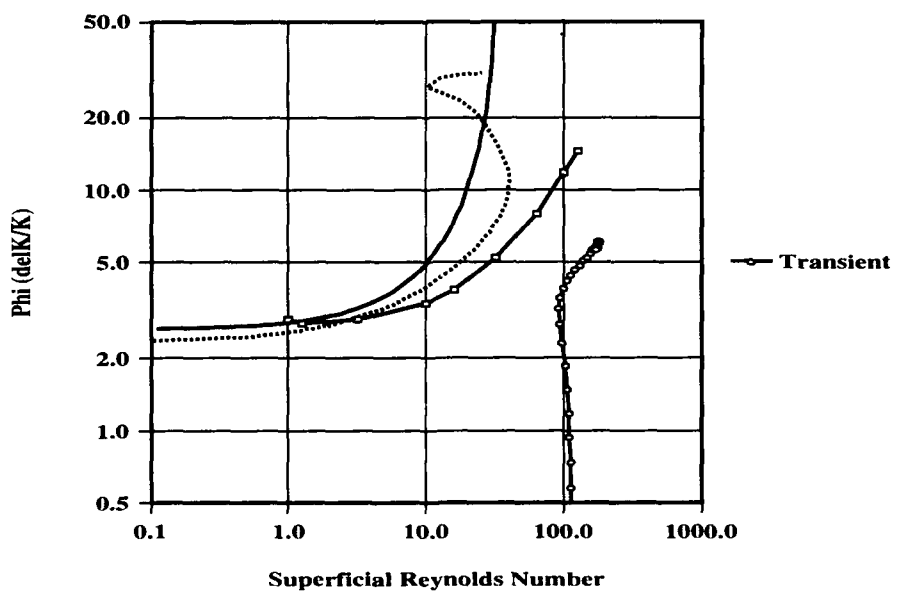
4.3 Other Issues

4.3.1 Sensitivity to TPA Inertia

The response of the engine system was found to be fairly sensitive to the modeled TPA moment of inertia. This is because the TPA inertia determines how much energy is required to accelerate the TPA; and, as seen in the results just presented, it is the TPA speed which largely determines the rate of coolant flow through the engine system. The control strategy used for the Fast Bootstrap Start was repeated for an engine system with twice the nominal TPA inertia; the effect of this change is presented in Figure 4.22. As expected, the transient progresses slower, reaching design conditions in about 9.0 *sec* rather then 6.0 *sec*. However, the flow stability during the transient is not significantly affected, so the general conclusions concerning the startup strategies should still be applicable.

Figure 4.22 Chamber Conditions for Larger TPA Inertia
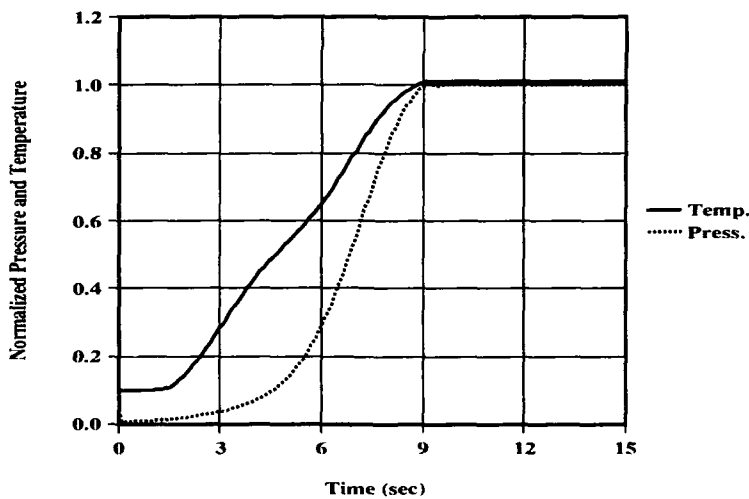
4.3.2 Reactivity Feedback

4.3.2.1 Nominal Operation

Another important issue associated with startup is the presence of reactivity feedback effects, especially due to the moderating effect of the hydrogen coolant introduced into the core. Figure 4.23 compares the total core reactivity, reactivity feedback, and control

drum worth for the Starter System Strategy. Of particular note is the ability of the MIT/SNL control law to maintain the desired reactivity despite very high rates of positive reactivity insertion and without estimating the anticipated feedback; this is most evident from approximately 2.0 to 2.8 *sec*.

Figure 4.23 Core Reactivity with Starter System
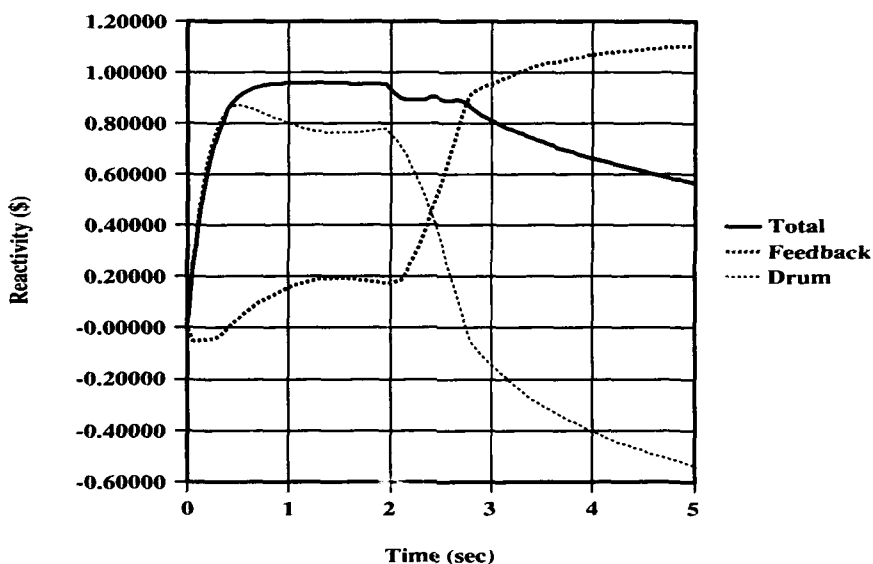
4.3.2.2 Control Drums Inoperable

With a starter system, the positive reactivity insertion due to hydrogen may be expected to present a problem if the starter cartridge fires but the control drums are inoperable. In this case, cold hydrogen will be introduced into the core causing a positive feedback effect which will in turn raise the reactor power. If the control drums cannot compensate the positive reactivity insertion, reactor control could be lost. A simulation of this case was run; the control drums were fixed at the engine idle position and all other controls were operated normally. No supervisory control is initiated although such control could be expected to mitigate any potential problems and eventually shut down the engine system. Figures 4.24 and 4.25 show the results of this simulation. As expected, the hydrogen introduced by the starter system causes an initial rise in core reactivity and

reactor power, but the chamber temperature does not change appreciably. Since sufficiently high temperature bleed flow is not available to bootstrap the engine system, the coolant flow rate quickly drops when the starter cartridge is expended, and the reactor power is rapidly reduced. The engine does not return to its initial critical state because a small amount of coolant flow will continue until the supervisory control shuts the pump discharge valve and turbine speed control valve. The continued hydrogen flow cools the moderator, thus reducing reactor power due to the positive moderator temperature coefficient. Note, though, that this simulation does not imply that the reactor is safe under all cases of control drum failure. If the control drums are initially rotated out during the startup (see Figure 4.23) but cannot be halted or reversed, an emergency shutdown system will likely be required. This will also be true for the Fast Bootstrap Start, but slightly more time may be available to initiate emergency action.

Figure 4.24 Core Reactivity with Control Drums Inoperable
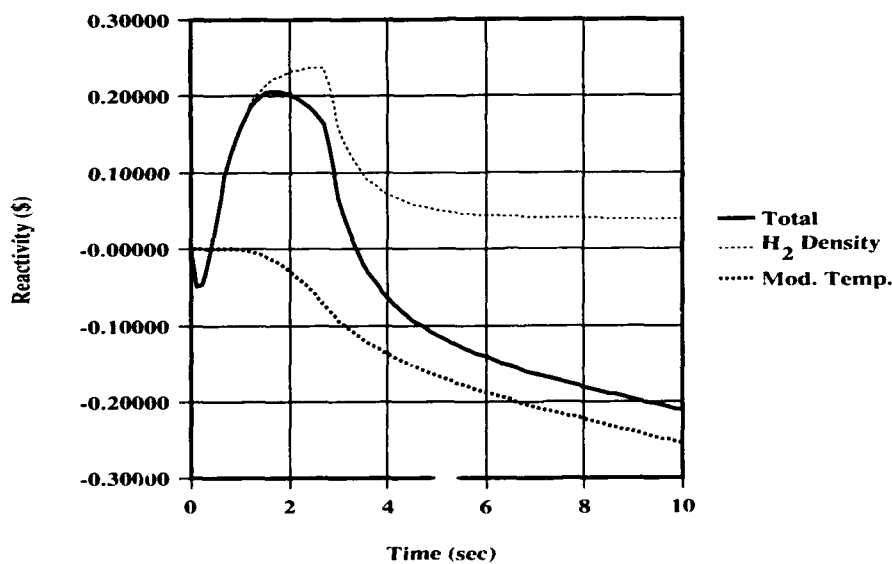
Figure 4.25 Power and Chamber Temperature with Drums Inoperable
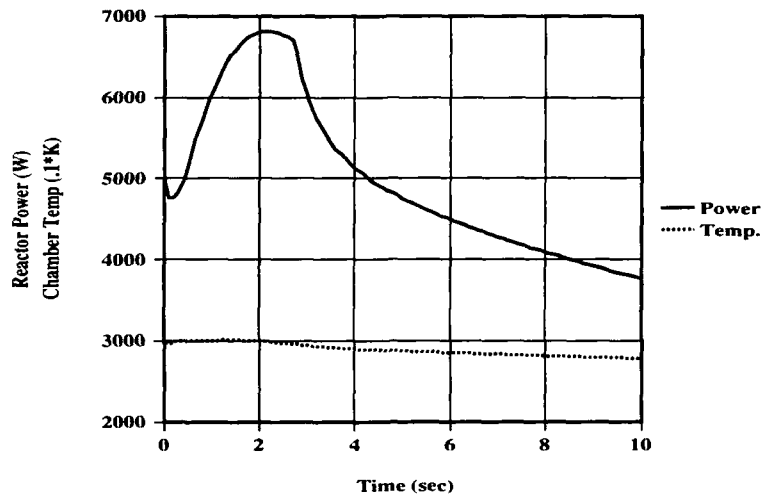
4.3.3 Controller Choice

4.3.3.1 General Factors

Both the Fast Bootstrap Start and Starter System Strategy meet the general design objectives specified; they each bring the PBR engine system from zero-flow/idle-power to full-flow/full-power very quickly while maintaining the coolant flow in the fuel elements well away from the currently understood flow instability boundaries. The choice of which general startup strategy to use and the details of the each strategy will likely depend on the issues presented in this thesis as well as many issues not covered. These include, but are not limited to: engine mission; ability to accommodate external disturbances and model uncertainties; fault tolerance; compatibility with the overall engine controller; transient thermal limits and stresses; and reactor safety. The reactor safety issue will involve questions such as the ability of the reactor to shut down safely during all phases of startup in the event of a loss of coolant, control drum failure as discussed above, or other accident.

4.3.3.2 Engine Mission

The engine mission can have a critical impact on the choice of the controller. For example, the engine mission may dictate that the system start as fast as possible, leading

68

to a starter system based strategy; or, if the mission requires that the engine must be restarted many times, a bootstrap start may be better since it does not require a starter cartridge for each anticipated startup. Figure 4.26 compares the total impulse generated by each startup strategy as a function of total propellant used. This plot shows that the starter system requires slightly more propellant (~3 kg) than the bootstrap start, but produces about 200 kN^*sec more impulse in the same time period. This information can help mission planners choose a particular startup strategy.

Figure 4.26 Comparison of Total Impulse vs. Mass Flow
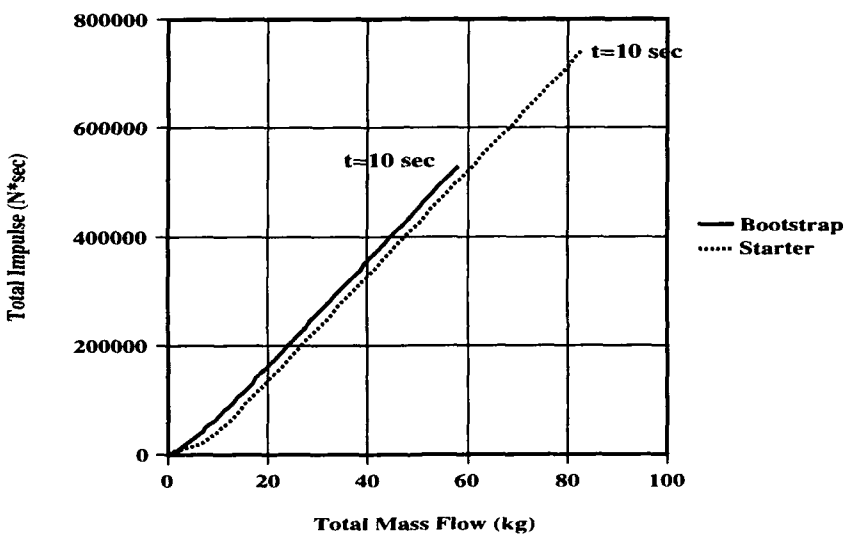
4.3.3.3 Flow Stability

Another issue which may impact the startup strategy choice is the flow stability through the fuel elements. The current understanding of the possible flow instability regime shows that either strategy should be able to maintain stable flow during the startup. However, the flow instability phenomena is not fully understood; it is possible that the operating conditions where flow instability might exist could actually be more encompassing than is currently believed. If this is the case, a starter system based strategy might be required since it has the ability to move the transient further away from the conditions which lead to possible flow instability.

Chapter 5 Summary, Conclusions, and Recommendations

5.1 Summary

This thesis has examined an important issue related to operation of particle bed reactor nuclear thermal propulsion engine systems which previously had not been addressed in detail. Analyses have shown that flow instability through the PBR fuel elements may occur during low flow but high temperature operation; such conditions are likely to be encountered during startup of PBR engine systems. An initial startup strategy confirmed that flow instability is an issue during startup. The objective of the thesis was to develop and analyze startup strategies which maintain stable flow through the fuel elements while reaching design conditions as quickly as possible.

The engine studies were conducted using a computer model of a nominal PBR engine system. The computer model utilized was an augmented version of the System Analysis Flow SIMulator (SAFSIM) program developed at Sandia National Laboratories to model the complex fluid mechanics, heat transfer, and reactor dynamics of nuclear thermal propulsion systems. The program was augmented by incorporating a portion of the Nuclear Thermal Propulsion SIMulator (NTPSIM) program which includes a simplified dynamic flow simulator. The combined program, dubbed SAFSIM+, provides an effective tool for modeling an entire NTP engine system. The PBR engine system studied is for a nominal orbital transfer vehicle mission. The system uses a hot bleed cycle; this cycle uses hot gas from the reactor chamber to drive the turbopump assembly which provides the propellant flow for the system. The reactor has a 19 element, 500 MW core; a simplified core power distribution is assumed. When operating at the design conditions of 7.0 MPa chamber pressure and 3000 K chamber temperature, this engine produces about 94 kN thrust at a specific impulse of 974 sec.

Two startup strategies were developed which satisfied the goal of maintaining stable flow through the PBR fuel element while reaching design conditions quickly. The Fast Bootstrap Start used a cubic reactor power to reactor flow coordination algorithm,

70

closed-loop chamber pressure control, turbine inlet temperature control, and bleed flow control. The engine system reached the design operating conditions in approximately 6.0 *sec* and maintained the reactor operation well away from the flow instability regime. A Starter System Strategy was also developed which uses a starter cartridge consisting of a small solid rocket motor to initially accelerate the TPA. This strategy resulted in a very fast start, with design conditions reached in only 2.8 *sec*. The flow stability was greatly enhanced since the starter system enables large coolant flow rates with low reactor coolant temperatures. The choice of engine startup strategy will depend on the results of these simulations as well as issues not addressed such as the engine system mission, performance robustness, fault tolerance, overall engine system control, and reactor safety.

5.2 Conclusions

In addition to the specific results just described, several general conclusions about startup strategies for a PBR engine system can be drawn from the results of the simulations conducted. For a bootstrap start, it was found that the relation used to coordinate reactor power with coolant flow rate is the dominant element of the control strategy which affects flow stability. By altering this relation to demand less power at lower coolant flow rates, the reactor exit temperature can be reduced during the initial phase of startup such that the PBR fuel element does not operate near the flow instability regime. All of the other elements of the control strategy had no appreciable effect on the flow stability. It was also found that increased bleed flow during the initial phase of startup is the only viable means of significantly increasing the speed of the system response. Simply increasing the speed control valve flow area or adding turbine inlet temperature control to assure the highest possible temperature at the turbine was insufficient for substantially increasing the system response speed. Finally, it was found that closed-loop chamber pressure control will be needed to force rapid convergence of the engine system to the design operating conditions. This appears to be due to the long time required for all system components to reach equilibrium temperatures; closed-loop control will also be needed to account for disturbances and model uncertainties.

A strategy based on a starter system was found to enable the system to reach design conditions in less than half the time required using a bootstrap start. However, achieving this rapid startup while preventing significant overshoots was found to require precise tailoring of the starter motor performance to ensure proper coordination of the bleed flow initiation and the burnout of the starter motor. The starter system was also found to be an effective mechanism for significantly enhancing flow stability during the startup. This aspect of a starter system based strategy may gain importance if the flow instability regime is later found to be more expansive than is currently believed.

In addition to the information on PBR engine systems, this thesis has demonstrated the utility of the SAFSIM+ program for modeling entire nuclear thermal propulsion engine systems. This program, made possible by the remarkable versatility of the SAFSIM program, was found to be quite robust. The program allowed the simulation of the modeled engine system under many different conditions, and allowed relatively easy and rapid reconfiguration of the base line model.

5.3 Recommendations

The knowledge gained from these studies should provide important information on particle bed reactor nuclear rocket engines to both engine designers and mission planners. However, several issues remain to be addressed. First, the startup strategies developed and the general conclusions which they provide will need to be reevaluated when the flow instability phenomenon is better understood. In addition, the flow stability analyses should include the actual operating conditions, including power generation profiles and coolant flow distributions, for each fuel element in the reactor core. Second, the startup strategies must be evaluated in terms of several specific aspects of the overall engine controller such as: performance robustness in the presence of external disturbances, model uncertainties, and sensor noise; fault tolerance in the case of sensor and/or actuator failures; and reactor safety, including the ability to shut down and remove decay heat during all phases of startup. Other aspects of PBR behavior, such as thermal stress during

rapid temperature transients, must also be studied and analyzed with respect to the startup strategy. Finally, it must be emphasized that much more extensive simulation and ground testing will be necessary to refine any control strategy and to learn more about particle bed reactor nuclear rocket engine behavior.

References

[B-1] Ball, Russell M. et. al. "Neutron Lifetime Measurements and Analysis in a Heterogeneous Thermal Reactor System." In *Proceedings of the Tenth Symposium on Space Nuclear Power and Propulsion.* CONF-930103. M. S. El-Genk and M. D. Hoover, eds. American Institute of Physics, New York, 1993.

[B-2] Benenati, R., K. J. Araj, and F. L. Horn. "Thermal Hydraulic Considerations for Particle Bed Reactors." *Space Nuclear Power Systems 1987.* Orbit Book Company, Malabar FL, 1988.

[B-3] Bernard, John A. *Startup and Control of Nuclear Reactors Characterized by Space-Independent Kinetics.* Report MITNRL-039. MIT Nuclear Reactor Laboratory, May 1990.

[B-4] Bussard, R. W. and R. D. DeLauer. *Nuclear Rocket Propulsion.* McGraw-Hill, New York, 1965.

[D-1] Dobranich, Dean. *SAFSIM Input Manual--A Computer Program for the Engineering Simulation of Flow Systems.* Report SAND92-0694. Sandia National Laboratories, September 1992.

[D-2] Dobranich, Dean. "System Analysis of P-Reactor Startup Transients Using SAFSIM." Internal Memo to David F. Beck. Sandia National Laboratories, 24 March 1992.

[D-3] Dobranich, Dean. Personal Communication, June 1992.

[G-1] Garrett Fluid Systems Division. Internal Memo to Grumman Electronic Systems Division. October 1988.

[G-2] Garrett Fluid Systems Division. Program ENGSIM Input File. October 1988.

[K-1] Kerrebrock, Jack L. and James Kalamas. "Flow Instability in Particle-Bed Nuclear Reactors." Paper AIAA 93-1758. AIAA/SAE/ASME/ASEE 29th Joint Propulsion Conference. Monterey, CA, June 1993.

[K-2] Koenig, Daniel R. *Experience Gained from the Space Nuclear Rocket Program (ROVER).* Report LA-10062-H. Los Alamos National Laboratory, May 1986.

[L-1] Lawrence, Timothy J. *Flow Instability Tests for a Particle Bed Reactor Nuclear Thermal Rocket Fuel Element.* S.M. Thesis, Department of Nuclear Engineering. Massachusetts Institute of Technology, May 1993.

[L-2] Lee, Stacey K. "Application of a General Fluid Mechanics Program to NTP System Modeling." In *Proceedings of the Tenth Symposium on Space Nuclear Power and Propulsion.* CONF-930103. M. S. El-Genk and M. D. Hoover, eds. American Institute of Physics, New York, 1993.

[L-3] Ludewig, Hans. "Particle Bed Reactor Nuclear Rocket Concept." *Nuclear Thermal Propulsion: A Joint NASA/DOE/DOD Workshop.* NASA Conference Publication 10079, 1991.

[M-1] Maise, George. "Flow Stability in the Particle Bed Reactor." Informal Report BNL/RSD-91-002. Brookhaven National Laboratory, January 1991.

[N-1] Norman, H. H. et. al. "NERVA Flight Engine Control System Design." *Nuclear Technology.* Vol. 15, September 1972.

[O-1] Overholt, David M. "High-Temperature Turbopump Assembly for Space Nuclear Thermal Propulsion." In *Proceedings of the Tenth Symposium on Space Nuclear Power and Propulsion.* CONF-930103. M. S. El-Genk and M. D. Hoover, eds. American Institute of Physics, New York, 1993.

[P-1] Parlos, Alexander G. and John D. Metzger. "A Framework for the Intelligent Control of Nuclear Rockets." In *Proceedings of the Tenth Symposium on Space Nuclear Power and Propulsion.* CONF-930103. M. S. El-Genk and M. D. Hoover, eds. American Institute of Physics, New York, 1993.

[P-2] Powell, James R. et. al. *Particle Bed Reactor Orbit Transfer Vehicle Concept.* Report AFAL-TR-88-014. Air Force Astronautics Laboratory, July 1988.

[S-1] Stafford, Thomas (Chairman). *America's Space Exploration Initiative: America at the Threshold.* Report of the Stafford Committee to the President of the United States, May 1991.

[S-2] Suzuki, David E. *Engine Cycle Analysis for a Particle Bed Reactor Nuclear Rocket.* Report PL-TR-91-3002. Phillips Laboratory, March 1991.

[T-1] True, William. "Gas Properties." Internal Memo to G. V. Perrin. Aerojet Tech Systems Company, 01 June 1988.

[W-1] Walton, James T. "Computer Subroutine NBS-PH2 for Thermodynamic Properties of Para-Hydrogen from NBS Monograph 168 (February 1981)." Computer Program LEW-155505. NASA Lewis Reasearch Center, 1992.

[W-2] Walton, James T. "Development of NASA/DOE NTP System Performance Models." In *Proceedings of the Tenth Symposium on Space Nuclear Power and Propulsion.* CONF-930103. M. S. El-Genk a⁻d M. D. Hoover, eds. American Institute of Physics, New York, 1993.

[W-3] Witter, Jonathan K. *Modeling for the Simulation and Control of Nuclear Reactor Rocket Systems.* Ph.D. Thesis, Department of Nuclear Engineering. Massachusetts Institute of Technology, June 1993.

Appendix A Modifications to SAFSIM Program

The SAFSIM+ program was developed by linking portions of the NTPSIM code with the basic SAFSIM code using the user-defined function capability of SAFSIM. However, in order to model the engine system, several slight modifications were made to the SAFSIM code. These changes, which did not include substantive changes to the SAFSIM solution method, are described below.

1) The variable 'relt' (relative time) was added to the input parameter list for the function UPR. This variable is used by the reactivity control algorithm.

2) The program was modified to allow for up to eight (8) inputs for the user-defined functions. The following changes were necessary:
   a) change 'ipntrf(maxf,6)' and 'iafnf(maxf,6)' to 'ipntrf(maxf,9)' and 'iafnf(maxf,9)', respectively, in appropriate common blocks.
   b) in SAFSIM4.FOR Block Data, add parameter maxf9=maxf*9 and change 'DATA IAFNF, L=1,6, MAXF6*0' to 'DATA IAFNF, L=1,9,MAXF9*0'.
   c) in SAFSIM1.FOR, subroutine INPUT, change 'DO L=1,6' to 'DO L=1,9'.

3) All references to 'UNIT=6' were changed to 'UNIT=16' since Unit 6 is the designation for the monitor (screen output).

4) Print flags were added for the print file output in subroutine PRNTCHK. The user-defined input block contains a line to specify which SAFSIM output files to create.

5) Made Function #130 (previously unused) User-Defined Function #6.

78

Appendix B SAFSIM+ User's Manual

B.1 Constructing a Model

Construction of a particular engine cycle model is accomplished by creating the appropriate SAFSIM reactor model, the NTPSIM systems model, and interfacing the two. The reactor model is created using the SAFSIM input file Blocks 1-17 (see SAFSIM input manual, Reference D-1). The NTPSIM systems model is created by assigning common variable names, modifying the UPDATE.F code, and creating Block 18 SAFSIM data input (see below). Furthermore, the CONTROL.F subroutine can be modified to model particular flow control algorithms. In addition to the standard SAFSIM output, user-defined output which includes the NTPSIM system output is written to the file SAFSIM.OU. The interface is accomplished via the SAFSIM system function controlled variables and the user-defined function subroutine within SAFSIMU.FOR. This subroutine, UFUN, incorporates the NTPSIM execution controller and passes the variable values between the two program components. Two integration options are available for the NTPSIM portion of the program: a variable step size stiff equation package and a fixed step size fourth-order Runge-Kutta integrator. The stiff equation package is generally much faster and is recommended unless difficulties arise in meeting the tolerances. The SAFSIM+ program is contained in twelve (12) source code listings which must be compiled and linked. The source codes are:

SAFSIM1.FOR	SAFSIM program modules
SAFSIM2.FOR	SAFSIM program modules
SAFSIM3.FOR	SAFSIM program modules
SAFSIM4.FOR	SAFSIM Block Data
SAFSIMU.FOR	SAFSIM user-defined subroutines
UPDATE.F	defines NTPSIM systems model
CONTROL.F	flow control algorithms
NTP1.F	NTPSIM element modules
NTP2.F	NTPSIM turbopump module
NTP3.F	Runge-Kutta integration routine and cubic spline estimator

DDEBDF.F	stiff equation solver package
UPH2EOS.F	NBS para-hydrogen properties routine

The programs should be linked using the following command (for UNIX systems):

f77 -w -align commons safsim1.f safsim2.f ...

It is recommended that a single object code be created using all optimizations for all the source codes except SAFSIMU.FOR, UPDATE.F, and CONTROL.F. Then, after these three subroutines are modified to create a specific engine model, they can be linked to the single object file. In this manner, an optimized executable code can be created much quicker when changes are made to any of these three files.

B.2 Assignment of Variables

Variables should be assigned in the following order:

tanks	differential variables (x)- pressure(p), pressure/temperature (p/t)
splitters	x- p, p/t
mixers	x- p, p/t
ducts	x- p, p/t
orifices	flows (w)- mass flow (w), flow*temperature (wt)
valves	x- area (a) w- w, wt
check valves	x- a w- w, wt
turbopump	x- a_PDV, t_pump_outlet, TPA_speed w- w_pump, wt_pump, w_turb_in, wt_turb_in, w_turb_out, wt_turb_out

Example: Hot Bleed Cycle (see Chapter 3)

Propellant Tank	TNK #1	p=x(1) p/t=x(2)
Starter System	TNK #2	p=x(3) p/t=x(4)
Pump Discharge	SP #1	p=x(5) p/t=x(6)

80

Bleed Mixer	MX #1	p=x(7) p/t=x(8)	
Starter Mixer	MX #2	p=x(9) p/t=x(10)	
Turbine Exhaust	DCT #1	p=x(11) p/t=x(12)	
Turbine Nozzle	OR #1		w(1), wt(1)
Turbine TCV	VALV #1	a=x(13)	w(2), wt(2)
Turbine SCV	CV #1	a=x(14)	w(3), wt(3)
Starter Valve	CV #2	a=x(15)	w(4), wt(4)
TPA		a_PDV=x(16) t_pmp_out=x(17) TPA_speed=x(18)	w_pump: w(5), wt(5) w_turb_in: w(6), wt(6) w_turb_out: w(7), wt(7)

B.3 Subroutine UPDATE.F Construction

Call statements to the appropriate subroutines for each element in the system should be made in the following order. Parameters should be passed using the appropriate COMMON variable names (e.g. x(j), xdot(j), w(k), wt(k), ...). Where appropriate, the input variable name from SAFSIM (e.g. 'wreac', 'wbleed') should be used.

For the turbopump:

call trbpmp(w_pump,wt_pump,p_p_in,t_p_in,p_p_out,t_p_out,t_pmp,dt_pmp,

   p_trb_in,t_trb_in,p_trb_out,s_trb,ds_trb,w_trb_in,wt_trb_in,w_trb_out,

  wt_trb_out,iflow_p,iflow_t,apdv,dpdva)

w_pump	flow through pump (and PDV)
wt_pump	flow times temperature through PDV
p_p_in	inlet element pressure to pump
t_p_in	inlet element temperature to pump
p_p_out	outlet element (after PDV) pressure for pump
t_p_out	outlet element (after PDV) temperature for pump
t_pmp	outlet temperature from pump
dt_pmp	derivative of t_pmp
p_trb_in	inlet element pressure to pump

t_trb_in	inlet element temperature to turbine
p_trb_out	outlet element pressure for turbine
s_trb	TPA speed
ds_trb	derivative of s_trb
w_trb_in	flow into turbine
wt_trb_in	flow times temperature into turbine
w_trb_out	flow out of turbine
wt_trb_out	flow times temperature out of turbine
iflow_p	index of pump fluid
iflow_t	index of turbine fluid
apdv	area of pump discharge valve
dpdva	derivative of apdv

Under 'resistor' elements-

For each orifice:

call orifice(p_in,t_in,p_out,t_out,w,wt,aor,iflow,istate)

p_in	inlet pressure
t_in	inlet temperature (use p/[p/t] if t not explicitly available)
p_out	outlet pressure
t_out	outlet temperature
w	flow through orifice
wt	flow times temperature
aor	area of orifice
iflow	index of fluid type
istate	state of fluid (1=ideal gas; 2=liquid)

For each valve: call valv(p_in,t_in,p_out,t_out,w,wt,av,dav,avc,ivnum,iflow,istate)

p_in	inlet pressure
t_in	inlet temperature
p_out	outlet pressure

t_out	outlet temperature
w	flow through valve
wt	flow times temperature
av	area of valve
dav	derivative of valve area
avc	commanded valve area
ivnum	index of valve
iflow	index of fluid type
istate	state of fluid (1=ideal gas; 2=liquid)

For each check valve:

call chckv(p_in,t_in,p_out,t_out,w,wt,av,dav,avc,icvnum,iflow,istate)

p_in	inlet pressure
t_in	inlet temperature
p_out	outlet pressure
t_out	outlet temperature
w	flow through check valve
wt	flow times temperature
av	area of check valve
dav	derivative of check valve area
avc	commanded check valve area
icvnum	index of check valve
iflow	index of fluid type
istate	state of fluid (1=ideal gas; 2=liquid)

Under 'capacitor' elements-

For each tank:

call tnk(time,itnum,p,pdot,pt,ptdot)

time	current simulation time
itnum	index of tank

p	tank pressure
pdot	derivative of tank pressure
pt	tank pressure/temperature
ptdot	derivative of tank pressure/temperature

For each splitter:

call splitter(wt_in,wt_1,wt_2,v_in,w_1,w_2,vsp,qin,dpsp,dptsp,iflow)

wt_in	flow times temperature into splitter
wt_1	flow times temperature of outlet #1
wt_2	flow times temperature of outlet #2
w_in	flow into splitter
w_1	flow of outlet #1
w_2	flow of outlet #2
vsp	splitter volume
qin	heat transfer into splitter
dpsp	derivative of splitter pressure
dptsp	derivative of splitter pressure/temperature
iflow	index of fluid

For each mixer:

call mxr(wt_1,wt_2,wt_out,w_1,w_2,w_out,vmix,qin,dpmix,dptmix,if1,if2,ifout)

wt_1	flow times temperature of inlet #1
wt_2	flow times temperature of inlet #2
wt_out	flow times temperature out of mixer
w_1	flow of inlet #1
w_2	flow of inlet #2
w_out	flow out of splitter
vmix	mixer volume
qin	heat transfer into mixer
dpmix	derivative of mixer pressure

dptmix	derivative of mixer pressure/temperature
if1	index of inlet #1 fluid
if2	index of inlet #2 fluid
ifout	index of outlet fluid

For each duct:

call dct(wt_in,wt_out,w_in,w_out,vduct,qin,dpduct,dptduct,iflow)

wt_in	flow times temperature into duct
wt_out	flow times temperature out of duct
w_in	flow into duct
w_out	flow out of duct
vduct	duct volume
qin	heat transfer into duct
dpduct	derivative of duct pressure
dptduct	derivative of duct pressure/temperature
iflow	index of fluid

Finally, the output variables from NTPSIM to SAFSIM should be assigned using the appropriate common variable names; the output variables are the values of the user-defined functions:

pinreac	reactor model inlet pressure
tinreac	reactor model inlet temperature
pout	reactor model outlet pressure
tout	reactor model outlet temperature

Example: Hot Bleed Cycle

```
c turbopump element
        call trbpmp(w(5),wt(5),x(1),x(1)/x(2),x(5),x(5)/x(6),x(17),
    &  xdot(17),x(9),x(9)/x(10),x(11),x(18),xdot(18),
    &  w(6),wt(6),w(7),wt(7),1,3,x(16),xdot(16))
```

85

```
c find mass flows through each 'resistor' element
c  turbine exhaust nozzle
          call orifice(x(11),x(11)/x(12),pamb,tamb,w(1),wt(1),aor(1),3,1)
c  turbine temperature control valve
          call valv(x(5),x(5)/x(6),x(7),x(7)/x(8),w(2),wt(2),x(13),
       &  xdot(13),atcvc,1,1,1)
c  turbine speed control valve
          call chckv(x(7),x(7)/x(8),x(9),x(9)/x(10),w(3),wt(3),x(14),
       &  xdot(14),ascvc,1,1,1)
c  starter system valve
          call chckv(x(3),x(3)/x(4),x(9),x(9)/x(10),w(4),wt(4),x(15),
       &  xdot(15),astvc,2,2,1)


c find time rates of change of pressure and pressure/temperature for
c  each 'capacitor' element
c  main coolant tank
          call tnk(simtime,1,x(1),xdot(1),x(2),xdot(2))
c  starter system tank
          call tnk(simtime,2,x(3),xdot(3),x(4),xdot(4))
c  pump discharge plenum
          call splitter(wt(5),wreac*x(5)/x(6),wt(2),w(5),wreac,w(2),
       &  vsp(1),0.0d0,xdot(5),xdot(6),1)
c  hot bleed and cool gas mixer
          call mxr(wbleed*tpbrex,wt(2),wt(3),wbleed,w(2),w(3),vmxr(1),
       &  0.0d0,xdot(7),xdot(8),1,1,1)
c  hydrogen and starter system exhaust mixer
          call mxr(wt(3),wt(4),wt(6),w(3),w(4),w(6),vmxr(2),0.0d0,
       &  xdot(9),xdot(10),1,2,3)
c  turbine exhuast duct
```

```
      call dct(wt(7),wt(1),w(7),w(1),vdct(1),0.0d0,
  &   xdot(11),xdot(12),3)


c assign output to SAFSIM
      pinreac = x(5)
      tinreac = x(5)/x(6)
      pmix  = x(7)
      tmix  = x(7)/x(8)
```

B.4 Data File Construction

The following data should be input under 'Block 18, User-Defined Data' in the SAFSIM
input file (see SAFSIM Input Manual, reference D-1).

Line 1

iprfm, iprht, iprrd, ipru, iplfm, iplht, iplrd, iplsys, ifcvfm, ifcvht, ifcvrd, ifcvsys

iprfm:	fluid mechanics print file flag (create=1, do not create=0)
iprht:	heat transfer print file flag
iprrd:	reactor dynamics print file flag
ipru:	user-defined output print file flag
iplfm:	fluid mechanics plot file flag
iplht:	heat transfer plot file flag
iplrd:	reactor dynamics plot file flag
iplsys:	system function controlled variable plot file flag
ifcvfm:	fluid mechanics function controlled variable print file flag
ifcvht:	heat transfer function controlled variable print file flag
ifcvrd:	reactor dynamics function controlled variable print file flag
ifcvsys:	system function controlled variable print file flag

Line 2

iout,ictrl,intalg,tsti,tstf

iout: number of NTPSIM timesteps per system timestep for runge-kutta integrator

ictrl: digital flow controller interval (number of system timesteps)

intalg: integration algorithm (stiff equation package=1, runge-kutta=2)

tsti: starter system initiation time

tstf: starter system finishing time

Line 3

tolr,tola

tolr   relative error tolerance for stiff equation package integrator

tola   absolute error tolerance for stiff equation package integrator

Line 4

gc,pamb,tamb

gc: gravitational constant (1.0 in mks units)

pamb: ambient pressure (Pa)

tamb: ambient temperature (K)

Line 5

nfluid,ntnks,nsps,nmxrs,ndcts,nors,nvlvs,ncvs

nfluid: number of fluids in system

ntnks: number of tank elements

nsps: number of splitter elements

nmxrs: number of mixer elements

ndcts: number of duct elements

nors: number of orifice elements

nvlvs: number of valve elements

ncvs: number of check valve elements

Repeat the next line (6) for each fluid type in system

Line 6

xk,r,gam,cp,cv,rho,taut

xk: gas flow constant, wtap ([kg/s][K^.5]/[m^2*Pa])

r: gas constant (J/kg/K)

gam: ratio of specific heats

cp: constant pressure specific heat (J/kg/K)

cv: constant volume specific heat (J/kg/K)

rho: liquid phase density (kg/m^3)

taut: thermal time constant of fluid (sec)

Repeat the next 2 lines (7-8) for each tank element in system

Line 7

tknam, tktf

tknam: tank name (up to 10 characters)

tktf: tank emptying time (sec)

Line 8

p_i,p/t_i

p_i: initial tank pressure (Pa)

p/t_i: initial tank pressure/temperature (Pa/K)

Repeat the next 2 lines (9-10) for each splitter element in system

Line 9

spnam,vsp

spnam: splitter name (up to 10 characters)

vsp: splitter volume (m^3)

Line 10

p_i,p/t_i

p_i: initial splitter pressure (Pa)

p/t_i: initial splitter pressure/temperature (Pa/K)

Repeat the next 2 lines (11-12) for each mixer element in system

Line 11

mxrnam,vmxr

mxrnam: mixer name (up to 10 characters)

vmxr: mixer volume (m^3)

Line 12

p_i,p/t_i

p_i: initial mixer pressure (Pa)

p/t_i: initial mixer pressure/temperature (Pa/K)

Repeat the next 2 lines (13-14) for each duct element in system

Line 13

dctnam,vdct

dctnam: duct name (up to 10 characters)

vdct: duct volume (m^3)

Line 14

p_i,p/t_i

p_i: initial duct pressure (Pa)

p/t_i: initial duct pressure/temperature (Pa/K)

Repeat the next 2 lines (15-16) for each orifice in system

Line 15

ornam,aor

ornam:	orifice name (up to 10 characters)
aor:	orifice area (m^2)

Line 16

w,wt

w:	initial orifice flow (kg/sec)
wt:	initial orifice flow times temperature (kg/sec*K)

Repeat the next 3 lines (17-19) for each valve in system

Line 17

vnam,tauv,vrl,vamn,vamx

vnam:	valve name (up to 10 characters)
tauv:	valve time constant (sec)
vrl:	maximum rate of change of valve area (m^2/sec)
vamn:	minimum valve area (m^2)
vamx:	maximum valve area (m^2)

Line 18

a_i

a_i:	initial valve area (m^2)

Line 19

w,wt

w:	initial valve flow (kg/sec)
wt:	initial valve flow times temperature (kg/sec*K)

Repeat the next 3 lines (20-22) for each check valve in system

Line 20

cvnam, taucv, cvrl, cvamn, cvamx

cvnam:	check valve name (up to 10 characters)
taucv:	check valve time constant (sec)
cvrl:	maximum rate of change of check valve area (m^2/sec)
cvamn:	minimum check valve area (m^2)
cvamx:	maximum check valve area (m^2)

Line 21

a_i

a_i:	initial check valve area (m^2)

Line 22

w, wt

w:	initial check valve flow (kg/sec)
wt:	initial check valve flow times temperature (kg/sec*K)

Enter the next 6 lines (23-28) for the turbopump

Line 23

taupv, pvrl, pvamn, pvamx, etapmx, tpaj, atrb, qnd, hnd, shpnd, etades, radius, uocdes

taupv:	pump discharge valve (PDV) time constant (sec)
pvrl:	maximum rate of change of PDV area (m^2/sec)
pvamn:	minimum PDV area; must be non-zero (m^2)
pvamx:	maximum PDV area (m^2)
etapmx:	maximum pump efficiency
tpaj:	turbopump assembly moment of inertia (N*m*sec^2)
atrb:	turbine effective flow area (m^2)
qnd:	pump design flow divided by TPA speed ([m^3/sec]/[rpm])
hnd:	pump design 'head' (pressure rise/density) divided by TPA speed squared

([Pa*m^3/kg]/[rpm^2])

shpnd: pump design shaft power divided by TPA speed cubed (W/rpm^3)

etades: turbine design efficiency

radius: turbine rotor tip radius (m)

uocdes: turbine design spouting ratio (tip speed/inlet mach speed)

Line 24

headn

headn: pump 'head' map; first value is number of data points, second value is abcissa starting value, third value is abcissa spacing, remaing values are map points

Line 25

horspn

horspn: pump required power map; same format as headn

Line 26

etadat

etadat: turbine efficiency map; same format as headn

Line 27

a_i,t_i,s_i

a_i: initial PDV area (m^2)

t_i: initial PDV outlet temperature (K)

s_i: initial TPA speed (rpm)

Line 28

w_p,wt_p,w_ti,wt_ti,w_to,wt_to

w_p: initial pump flow (kg/sec)

wt_p: initial pump flow times temperature (kg/sec*K)

93

w_ti: initial turbine inlet flow (kg/sec)

wt_ti: initial turbine inlet flow times temperature (kg/sec*K)

w_to: initial turbine outlet flow (kg/sec)

wt_to: initial turbine outlet flow times temperature (kg/sec*K)

A third MIT/SNL based neutronic power control law has been added to the programmed reactivity options. This control law includes estimation of the current reactivity and delay group precursor concentrations based on measured power. Control drum rotations are also included. If this control law is used, the following data should be used in 'Block 13, Reactor Dynamics Data' (see SAFSIM Input Manual):

Line 95

auxrd(kaux=1,3)

auxrd(1)   element flow rate (kg/sec); this variable is functioncontrolled

auxrd(2)   flow matching initiation time (sec)

auxrd(3)   maximum drum worth; this variable is function-controlled

Line 110

xtpr(kx=1,10)

xtpr(1)   rated (target) neutron power (W)

xtpr(2)   rated reactor flow rate (kg/sec)

xtpr(3)   fastest allowed reactor period (sec)

xtpr(4)   maximum allowed drum rotation rate (rad/sec)

xtpr(5)   number of system timesteps per reactivity control interval

xtpr(6)   proportional feedback gain

xtpr(7)   reactivity feedback estimation flag   (estimate<0.5 [not functional],

                                                     do not estimate>0.5)

xtpr(8)   number of control intervals for projecting power

xtpr(9)   initial reactor neutron power (W)

xtpr(10)   commanded power option flag (currently, linear power/flow matching<0.5

                                            cubic power/flow matching>0.5)

Line 110a

ypr(1)

ypr(1)   initial drum position (radians)

B.5 Output File

User-Defined data is written to the file SAFSIM.OU. Currently, the following data is output at each print interval in the order specified. The choice of outputs is tailored to the needs of the engine studies; variables are based on the engine cycle described in Chapter 3.

system time	time
reactor inlet pressure	x(5)
chamber pressure	presn(56)
chamber temperature	tn(56)
pump flow rate	w(5)
reactor flow rate	floe(1)*19
cold flow rate to mixer	w(2)
main nozzle flow rate	floe(58)*19
hot bleed flow rate	floe(59)*19
turbine hydrogen flow rate	w(3)
starter system flow rate	w(4)
total turbine flow rate	w(6)
turbine inlet temperature	x(9)/x(10)
SCV effective flow area	x(14)
TPA speed	x(18)
turbine exhaust pressure	x(11)
turbine exhaust temperature	x(11)/x(12)

turbine nozzle flow rate	w(1)
fuel element inlet temp.	tn(39)
fuel element outlet temp.	tn(44)
element inlet Reynolds #	calculated from floe(39) and viscosity at node 39
reactor power	rdne(1)*19
reactivity ($)	react(1)/beta(1)
feedback reactivities ($)	dreaci(j,1)/beta(1), for j=1,6
reactivity rate commanded	ypr(1,4)
control drum angle (deg)	ypr(1,1)*180/π
chamber specific heat ratio	cpe(57,0)/cve(57,0)
chamber gas constant	rgasm(57)

Additionally, more general data output is possible. This can be achieved by uncommenting the appropriate lines in the user-defined output subroutine, UOUT. Data is limited to the time plus fifty (50) output variables by the format statement. The output values are assigned in the following order:

For each tank element in system

p,t

p: tank pressure (Pa)

t: tank temperature (K)

For each splitter element in system

p,t

p: splitter pressure (Pa)

t: splitter temperature (K)

For each mixer element in system

p,t

p: mixer pressure (Pa)

t: mixer temperature (K)

For each duct element in system

p,t

p: duct pressure (Pa)

t: duct temperature (K)

For each orifice in system

w

w: orifice flow (kg/sec)

For each valve in system

a,w

a: valve area (m^2)

w: valve flow (kg/sec)

For each check valve in system

a,w

a: check valve area (m^2)

w: check valve flow (kg/sec)

For the TPA

a_pdv,t_pmp,s_trb,w_pmp,w_trb,hpmp,shp

a_pdv: PDV area (m^2)

t_pmp: pump outlet temperature (K)

s_trb: TPA speed (rpm)

w_pmp: pump flow (kg/sec)

w_trb: *turbine flow (kg/sec)*

hpmp: pump 'head' (pressure rise/density) (Pa/[kg/m^3])

shp: shaft power (W)

For the neutronics (based on MIT/SNL control law #3)

pwr,w_react,rho,drhodt,drum

pwr: reactor neutron power (W)

w_react: element flow rate (kg/sec)

rho: observed reactivity

drhodt: commanded time rate of change of reactivity

drum: drum position (degrees)

Appendix C Additional Results for Fast Bootstrap Start

Figure C.1 Reactor Power and Coolant Flow Rate
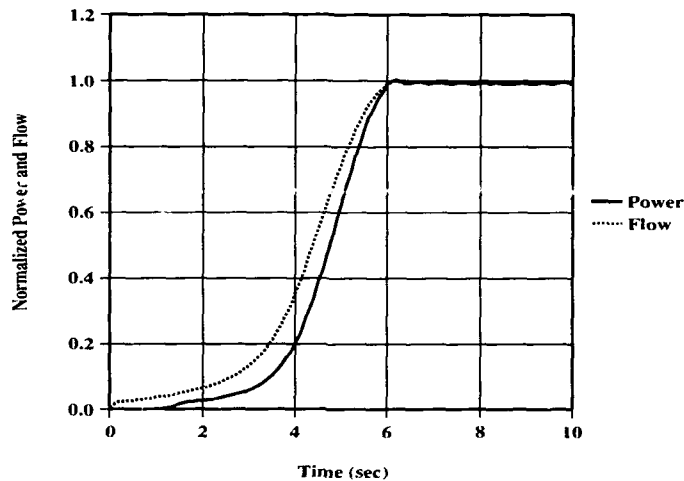

Figure C.2 Reactor Power vs. Reactor Coolant Flow Rate
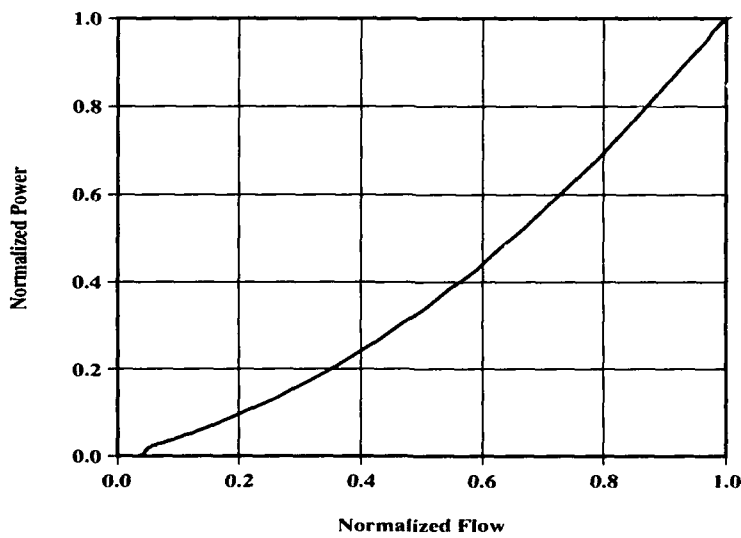
Figure C.3 Chamber and Turbine Inlet Temperature
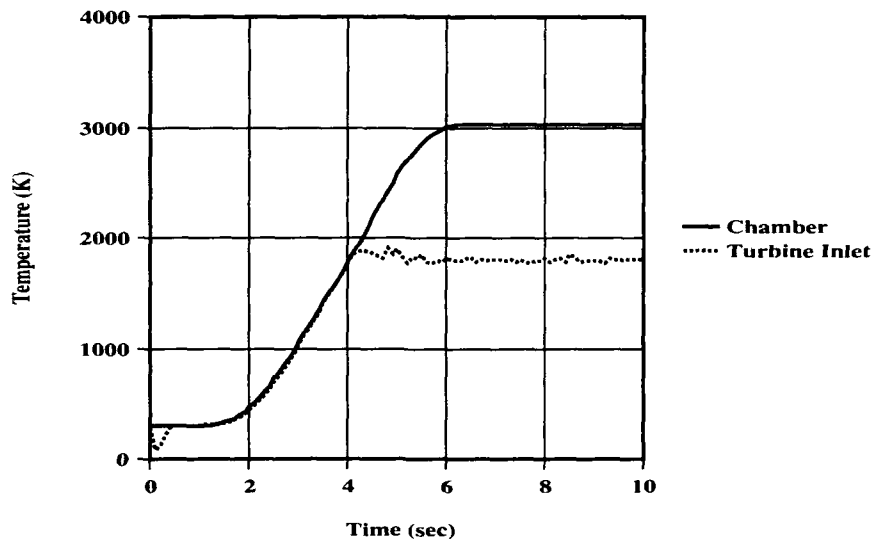
Figure C.4 Control Drum Position
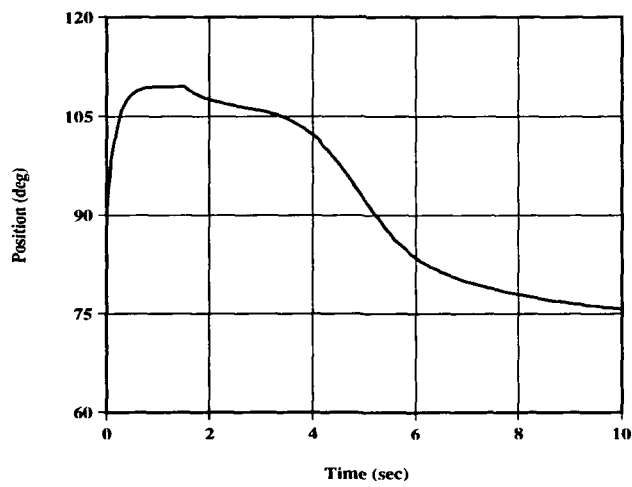
Figure C.5 Core Reactivity
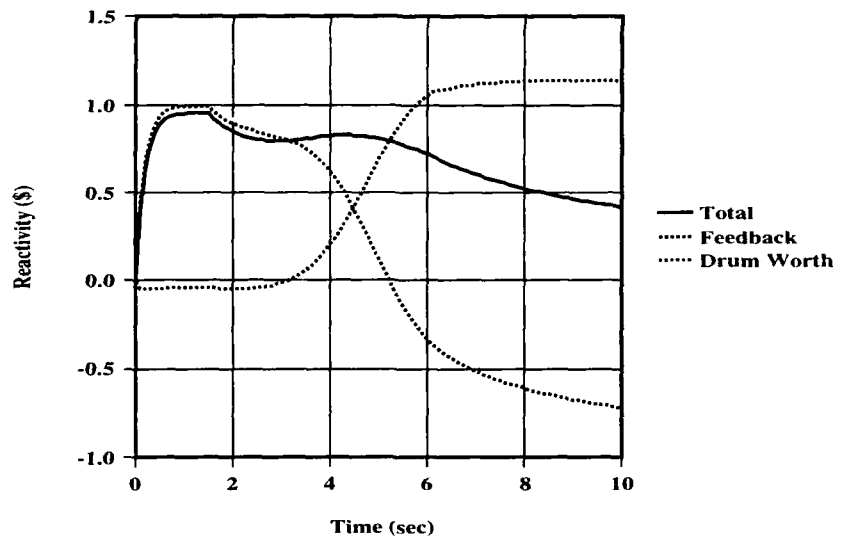
Figure C.6 SCV Flow Area

101
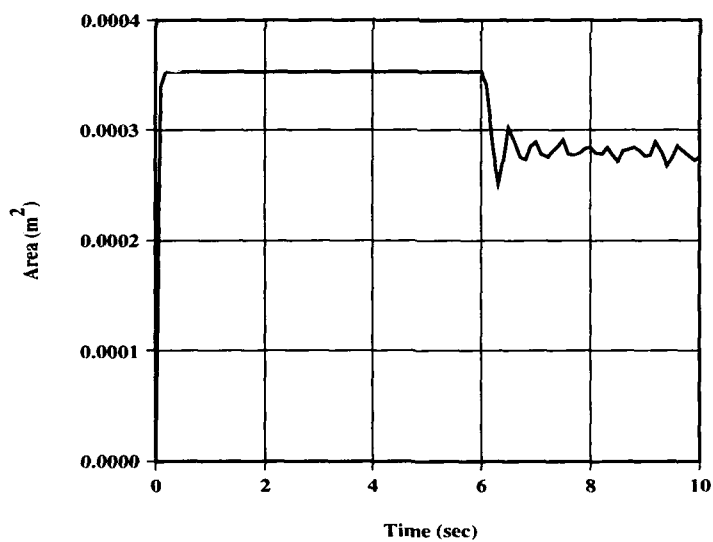
Figure C.7 TPA Speed
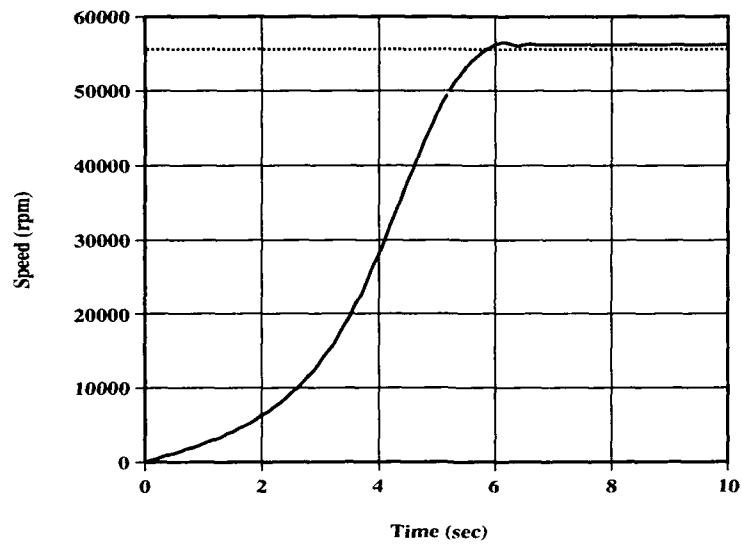
Appendix D Additional Results for Starter System Strategy

Figure D.1 Reactor Power vs. Reactor Coolant Flow Rate
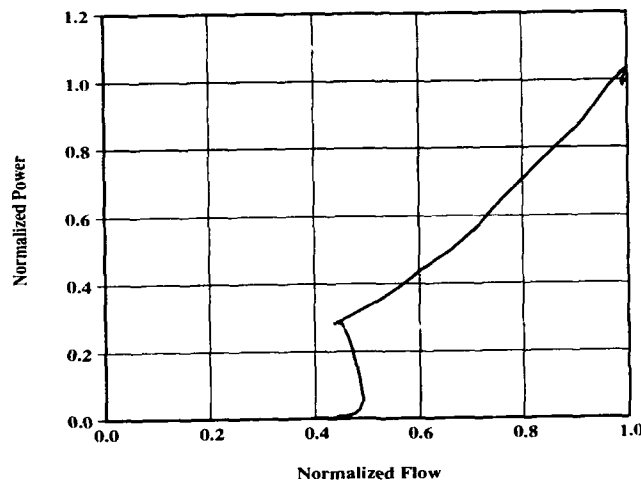
Figure D.2 Chamber and Turbine Inlet Temperature
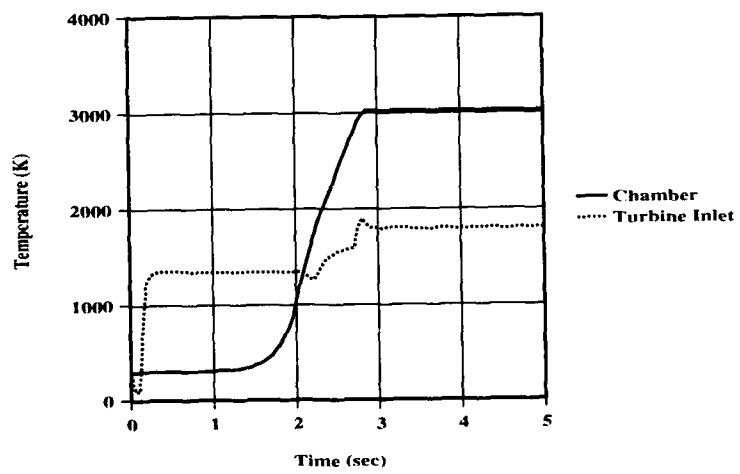
Figure D.3 Control Drum Position